UNIVERSITA' DI NAPOLI FEDERICO II

DOTTORATO DI RICERCA IN BIOCHIMICA

E BIOLOGIA CELLULARE E MOLECOLARE

XXVI CICLO

Anna Sirico

DISSECTING THE MOLECULAR MECHANISMS AT THE BASIS OF IMPAIRED p63 TRANSCRIPTIONAL ACTIVITY IN AEC SYNDROME

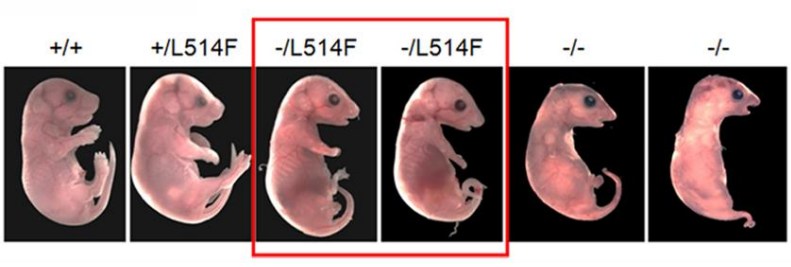

Academic Year 2012/2013

UNIVERSITA' DI NAPOLI FEDERICO II

DOTTORATO DI RICERCA IN BIOCHIMICA

E BIOLOGIA CELLULARE E MOLECOLARE

XXVI CICLO

DISSECTING THE MOLECULAR MECHANISMS AT THE BASIS OF IMPAIRED p63 TRANSCRIPTIONAL ACTIVITY IN AEC SYNDROME

Candidate

Anna Sirico

Tutor **Coordinator**

Prof.ssa Caterina Missero **Prof. Paolo Arcari**

Academic Year 2012/2013

RINGRAZIAMENTI

Nei ringraziamenti sarò davvero molto breve, le persone a cui va il mio pensiero spero lo sappiano già ampiamente.
Ringrazio tutti coloro che hanno contribuito alla mia crescita scientifica e non da meno a quella personale.
Ringrazio le persone che credono in me ogni giorno, al di là delle distanze.
Ringrazio tutti i componenti del laboratorio che mi ha ospitato in questi tre anni.
Ringrazio gli amici vecchi e nuovi.

Sarò per sempre grata, infine, alla mia famiglia.

SUMMARY

AEC (***A**nkyloblepharon- **E**ctodermal defects- **C**left lip/palate syndrome*) syndrome is an autosomal dominant disorder mainly characterized by ectodermal dysplasia, skin erosions and cleft lip and/or palate. This disorder is caused by missense mutations in the Sterile Alpha Motif (SAM) domain and frameshift mutations in the Post-SAM (PS) domain of the transcription factor p63, a crucial regulator of embryonic development of stratified epithelia.

To fully understand the molecular mechanisms associated with the pathogenesis of AEC syndrome, we analyzed transcription ability and DNA binding capacity of AEC causative p63 mutant proteins in heterologous system. L514F, G534V, C519R, D544Y, mutations involving SAM domain, and E570fsX94 and N620fsX44, mutations in the PS domain, showed an impaired transactivation ability consequent to a reduced DNA binding capacity, both when transfected alone and in combination with wild-type protein.

To further explore the role of the two C-terminal domains of p63α isoform, that are involved in AEC syndrome, we obtained two deletion p63 mutants that lack alternatively SAM (p63ΔSAM) or PS (p63ΔPS) domains, and tested transactivation and DNA binding. We found that the SAM domain, but not the PS one, is strongly involved in these functions, since the deletion of the whole domain impaired transactivation and DNA binding ability, in spite of an intact DNA binding domain of p63.

To test the physiological significance of our findings, we analyzed the effect of an endogenous L514F p63 mutant in primary keratinocytes.

To this aim we took advantage of a conditional knock-in mouse model ($p63^{+/floxL514F}$) recently generated in our laboratory. In accordance with previous results, also in its natural context AEC p63 mutant showed a reduced DNA binding and decresed expression levels of different p63 target genes, such as Fgfr2, IRF6, Dsc3, Dsp, Krt5 and Krt14, both in homozygous and in heterozygous mutant keratinocytes.

Finally, we tested the effects of L514F p63 mutant *in vivo* mating $p63^{+/-}$ mice with knock-in $p63^{+/L514F}$ ones, previously generated in our laboratory that closely resembles the human disease but died soon after birth for cleft palate, to obtain $p63^{-/L514F}$ mice. At E18.5 we observed epidermal, limbs and craniofacial development defects and with ChIP

assays on E14.5 embryos skin an impairement in DNA binding ability in $p63^{-/L514F}$ mice was confirmed.
These results shed light on the mechanisms underlying AEC syndrome, since all the analyzed mutant p63 proteins show an impairment in DNA binding ability, moreover this reduction is observed in heterozygous keratinocytes suggesting that L514F p63 mutant acts in a dominant negative manner, forming with wild-type proteins tetramers not well working. Using p63 deletion mutants we demonstrate that an intact SAM domain is required for transactivation and DNA binding ability in ΔNp63α context, while large rearrangements of PS domain, such as frameshift mutations but not whole domain deletion, show same effects, suggesting that this domain is not required for the described p63 functions. Finally, with *in vivo* experiments we demonstrate the crucial role of α-isoform of p63 in epidermal, limbs and craniofacial development and that its mutations, although in the presence of intact β and γ isoforms, strongly impaired development and DNA binding capacity, which explains pathogenesis of AEC syndrome.

RIASSUNTO

La sindrome AEC (Ankyloblepharon- Ectodermal defects- Cleft lip/palate syndrome) è una malattia autosomica dominante, caratterizzata principalmente da displasia ectodermica, erosioni cutanee e labioschisi e/o palatoschisi. Questo disordine è causato da mutazioni missenso localizzate nel dominio Sterile Alpha Motif (SAM) e mutazioni frameshift nel dominio post-SAM (PS) del fattore di trascrizione p63, un regolatore fondamentale dello sviluppo embrionale degli epiteli stratificati.

Per meglio comprendere i meccanismi molecolari associati alla patogenesi della sindrome AEC, abbiamo analizzato la capacità trascrizionale e di legame al DNA di mutanti di p63 causativi della patologia in questione in un sistema eterologo. L514F, G534V, C519R, D544Y, mutazioni che coinvolgono il dominio SAM, e E570fsX94 e N620fsX44, mutazioni nel dominio PS, hanno mostrato una ridotta capacità di transattivazione conseguente ad una ridotta capacità di legare il DNA, sia quando trasfettate da sole che in combinazione con la proteina wild-type.

Per esplorare ulteriormente il ruolo dei due domini C-terminali dell'isoforma α di p63 coinvolti nella sindrome AEC, abbiamo ottenuto due mutanti di delezione di p63 che mancano alternativamente del dominio SAM (p63ΔSAM) o PS (p63ΔPS) e ne abbiamo testato transattivazione e legame al DNA. Abbiamo così trovato che il dominio SAM, ma non il PS, è coinvolto in queste funzioni, in quanto la sua delezione compromette fortemente le attività di ΔNp63α, a dispetto di un dominio di legame al DNA ancora intatto.

Per testare il significato fisiologico delle nostre scoperte, abbiamo analizzato l'effetto del mutante di p63 L514F endogeno in cheratinociti primari.

A questo scopo abbiamo approfittato di un modello murino condizionale knock-in ($p63^{+/floxL514F}$) recentemente generato nel nostro laboratorio. In accordo con i risultati precedentemente ottenuti, anche nel suo contesto naturale il mutante di p63 causativo della sindrome AEC ha mostrato un ridotto legame al DNA e diminuiti livelli di espressione di diversi geni bersaglio di p63, come Fgfr2, IRF6 , Dsc3, Dsp, Krt5 e Krt14, sia in cheratinociti omozigoti per la mutazione che in quelli eterozigoti.

Infine, abbiamo testato gli effetti della mutazione L514F di p63 *in vivo* accoppiando topi $p63^{+/-}$ con quelli knock-in $p63^{+/L514F}$, precedentemente generati nel nostro laboratorio, i quali ricapitolano la patologia umana ma muoiono poco dopo la nascita per palatoschisi, per ottenere topi $p63^{-/L514F}$. Allo stadio embrionale E18.5 abbiamo riscontrato difetti nello sviluppo cranio-facciale, dell'epidermide e degli arti e tramite saggi di immunoprecipitazione della cromatina effettuati su pelle di embrioni a E14.5 abbiamo confermato una riduzione della capacità di legame al DNA in topi $p63^{-/L514F}$.
Questi risultati chiariscono i meccanismi sottostanti la sindrome AEC, dal momento che tutte le proteine di p63 mutanti analizzate mostrano un compromessa capacità di legame al DNA, questa riduzione si osserva nei cheratinociti omozigoti per la mutazione ma anche negli eterozigoti, ciò suggerisce che quanto meno il mutante L514F agisce da dominante negativo, formando con la proteina wild-type tetrameri non funzionanti. Utilizzando mutanti di delezione di p63 abbiamo dimostrato che un dominio intatto SAM è richiesto per la corretta transattivazione e per il legame al DNA nel contesto della ΔNp63α, mentre grandi riarrangiamenti del dominio PS, come mutazioni frameshift ma non la delezione totale del dominio, mostrano gli stessi effetti, suggerendo che questo dominio non è richiesto per le funzioni di p63 sopra descritte. Infine, con esperimenti *in vivo* abbiamo dimostrato il ruolo cruciale dell' isoforma α di p63 nello sviluppo degli epiteli stratificati, degli arti e nello sviluppo cranio-facciale, e che mutazioni che la coinvolgono, pur in presenza di isoforme di p63 β e γ funzionanti, compromettono fortemente il suo ruolo di fattore trascrizionale, spiegando le basi della patogenesi della sindrome AEC.

INDEX

1. INTRODUCTION

2. MATERIALS AND METHODS

LIST OF FIGURES

1. INTRODUCTION

1.1 Epidermis and its development

The skin is the first barrier that protects the body from hazardous substances such as chemical, infectious, and mechanical stressors. Mammalian skin has two major compartments, the dermis and the epidermis, which are separated by a basement membrane (1). This two compartments function cooperatively and together are responsible for the development of epidermal appendages, including hair follicles and mammary glands (2). The epidermis is the outermost component of the skin and consists of four distinct cell layers, from bottom to top: the basal, the spinous, the granular and the stratum corneum or cornified layer (1-Fig. 1). The stratified squamous epithelium is maintained by cell division within the basal layer. Differentiating cells slowly move outwards toward the stratum corneum, where anucleate corneal cells are continuously shed from the surface (desquamation). In normal skin the rate of production equals the rate of loss, taking about two weeks for a cell to migrate from the basal cell layer to the top of the granular cell layer, and an additional two weeks to cross the stratum corneum (3).

The epidermis, like other stratified epithelia, has a self-renewing capacity throughout life, and this continuous turnover is mediated by stem cells in the basal layer of the interfollicular epidermis (4) and in the bulge region of the hair follicle (5). Epidermal stem cells give rise to daughter stem cells and to transit amplifying cells, which constitute the major cell type in the basal layer of the developing and mature epidermis (4, 6). After a few rounds of cell division, transit amplifying cells permanently exit from the cell cycle, and initiate a terminal differentiation program. Further epidermal maturation occurs when spinous cells differentiate into granular cells and finally, cornified cell envelopes are assembled by cross-linking of structural proteins and lipids (7). The process of keratinocyte differentiation in mature epidermis mimics the initial development and maturation of keratinocytes during embryogenesis. Epidermal keratinocytes derive from the single-layered surface ectoderm and develop when the underlying mesenchyme releases an inductive signal (8). So epidermal

development and differentiation are multi-step processes, which involve the sequential action of many molecules.
One gene that is essential for early stages of skin development is the transcription factor p63 (9,10,11).

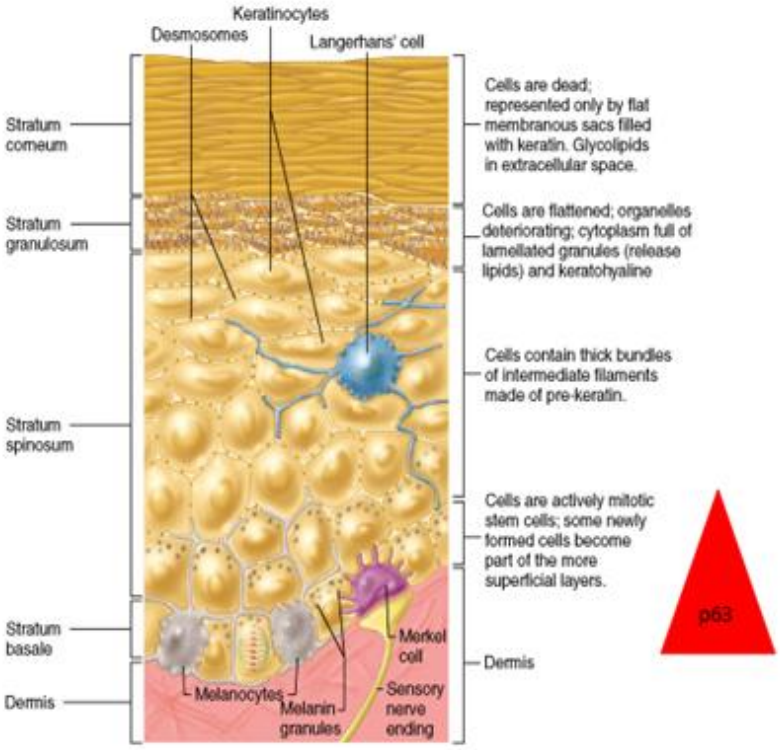

Figure 1: Epidermis. Mammalian skin consists of the epidermis and dermis, separated by a basement membrane. The epidermis is a stratified squamous epithelium composed by, from bottom to top: stratum basale consisting of proliferating, transit- amplifying cells interspersed to epidermal stem cells, stratum spinosum, stratum granulosum and corneum. p63 is predominantly expressed in the basal layer of the epidermis, it is downregulated upon keratinocyte differentiation. Copyright 2001 Benjamin Cummings, an imprint of Addison Wesley Longman, Inc.

1.2 The transcription factor p63

p63 belongs to the p53 gene family consisting of three genes, p53, p63, and p73, that show significant sequence homology (12) and share three functional domains commonly found in transcription factor: an N-terminal transactivation domain which shares 25% homology with N-terminal part of p53, a central DNA binding domain which shares 65% of homology with the corresponding p53 domain and C-terminal tetramerization domain, which shares 35% of homology with the oligomerization domain of p53. In addition, all family members share some biological functions and bind to a canonical p53-binding site, thus controlling the expression of a subset of p53 target genes (12,13). p63, p53 and the third member p73, constitute a family of key transcriptional regulators in cell growth, differentiation and apoptosis.

While p53 is a major player in tumorigenesis (14), p63 and p73 appear to have pivotal roles in embryonic development (9,15). More in detail, p63 has a crucial role in embryonic development of stratified epithelia.

The p63 gene encodes a tetrameric transcription factor, of 16 exons located on chromosome 3q28, that can be expressed in at least six isoforms with widely different transactivation potential that share an identical DNA binding domain (16). Alternative transcription start sites (TSS) give rise to transactivation (TA) isoforms, encoding proteins with a canonical transactivation domain similar to p53, and ΔN isoforms containing an alternative transactivation domain (17, 16). Due to the absence of the typical N-terminal transactivation domain, ΔNp63 isoforms were initially believed to be transcriptionally inactive (16). Consistent with this initial prediction and since ΔNp63 isoforms retain the oligomerization and DNA binding domains, it is plausible that they act as dominant-negative inhibitors of TAp63 isoforms during epidermal development (11). A possible mechanism is due to the formation of transcriptionally inactive ΔN-TA heterotypic or homotypic tetramers (composed of either all-TA or all-ΔN monomers) that compete for the same DNA binding sites. ΔNp63 isoforms, however, are also able to induce target gene expression in cell lines and in primary keratinocytes, suggesting that ΔNp63 isoforms may perform multiple roles in the developing and mature epidermis (18,

19, 20). This is possible thanks to existence of two cryptic transactivation domains in ΔNp63 isoforms: a region encompassing the first 26 N-terminal amino acids named TA* domain and a prolin rich sequence corresponding to exon 11/12 (21).

In addition to the use of two different transcription start sites the complexity of p63 transcripts is increased by alternative splicing at the C-terminus, which gives rise to three different carboxyl termini, termed α, β, and γ (16). Only p63α isoforms, the longest p63 isoforms, contain a sterile alpha motif (SAM) domain (22, 23) and a post-SAM (PS) domain, which has been shown to function as a transcriptional inhibitor domain (TID) (21,24- Fig. 2).

The most abundant isoform ΔNp63α is expressed from cells of the basal layer of epidermis (16). ΔNp63α is one of the first genes to be specifically expressed in the surface ectoderm prior to Krt5 and Krt14 expression at E7.5-E8 and it continues to be expressed during skin development and in the basal proliferative layer in postnatal life (11, 25, 16). Whereas p63 is predominantly expressed in the basal layer of the epidermis, it is downregulated upon keratinocyte differentiation both in vitro and in vivo (26-31, 10- Fig. 1). In the basal layer, p63 is mainly involved in maintaining cell proliferation and cell adhesion (13, 11, 32, 33). It has been proposed that p63 plays a dual role in keratinocyte differentiation, as it is required for initiating epithelial stratification (11, 28, 33), whereas concurrently it inhibits the expression of some differentiation markers (19, 28).

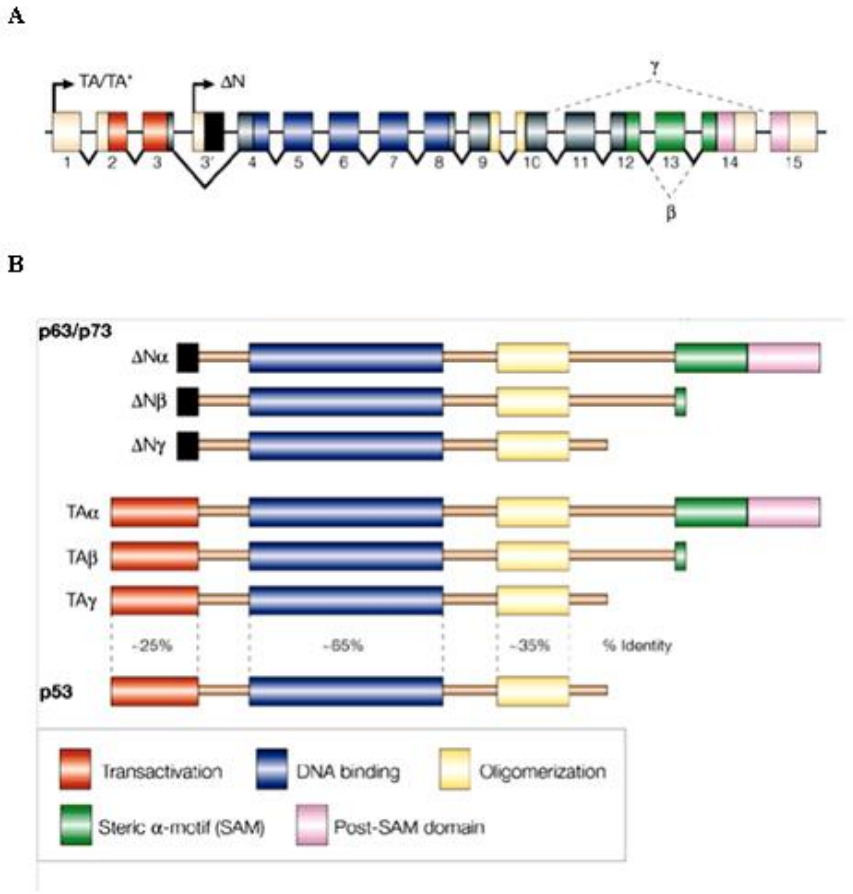

Figure 2: p63 gene. (A) Structure of p63 gene with the different transcription start sites and C-terminus isoforms. (B) Comparison between p53, p63 and p73 proteins. The schematic structure of p63 and p73 is shown, including the transactivation domain, the DNA-binding domain, the oligomerization domain, the steril α motif (SAM) and the post-SAM domain (PS). The percentage of identity is indicated for each domain. (Adapted from Yang et al., On the shoulders of giants:p63, p73 and the rise of p53, TRENDS in Genetics, 2002)

1.3 The α-terminus

The C-terminal region of p63 and p73 is coded by three (p63) to four (p73) additional exons, not present in p53, that are subject to alternative splicing, yielding different proteins with different biological properties (16, 34, 35). The full-length α-isoform of p63 and p73 contains at the C-terminal a structural module known as sterile-alpha motif (SAM) and a post-SAM (PS) domain, which is absent in all other isoforms.
While p63β and p63γ display p53-like functions, p63α has little or no p53 like activity, suggesting that these C-terminal domains could be responsible for those functional differences (23, 36).

- SAM domain:
SAM domains are among the most abundant protein-protein interaction motifs (~70-amino acid) in organisms from yeast to humans (more than 1300 SAM-containing proteins in all genomes). Although SAM domains adopt similar domain structure, they are remarkably versatile in their binding properties. Such versatility earns them functional roles in myriad biological processes.
SAM domains are usually found in the context of larger multidomain proteins and may be found in all cellular compartments, implying roles in complex and wide-ranging cellular processes. These domains are found in a wide variety of proteins involved in cell signaling, in developmental regulation, signal transduction and transcriptional activation, and repression (38) including the Eph family of tyrosine kinase receptors (39, 40), the ETS family of transcription factors (41), polyhomeotic proteins (41), diacylglycerol kinases (42), liprins (43), the connector enhancer of KSR (44), serine-threonine kinases, adapter proteins, and others (38). Defects in the SAM domains of proteins have been observed in a number of human diseases (45-47), for example chromosomal translocation of the ETS family transcriptional regulator TEL (translocation Ets leukemia), a SAM-domain containing protein, has been frequently linked to human leukemias and it is thought that the diseases arise because SAM-mediated oligomerization constitutively activates mitogenic proteins (48-50) and missense mutations in the SAM domain of p63 cause AEC (Ankyloblepharon Ectodermal defects Cleft lip/palate) syndrome

(OMIM 106260), a rare autosomal dominant disorder characterized by ectodermal dysplasia and orofacial clefting, and Rapp Hodgkin syndrome (RHS, OMIM 129400), very similar to AEC one, for a still unknown reason.

The common mechanism of interaction is homo- and hetero-oligomerization among similar SAM domains (51, 52), but it can also mediate intermolecular association with nucleic acids, lipids or other proteins not containing SAM domain (38-53).

The SAM domain in p63 is encoded by exons 13 and 14 in the p63α gene (16). The solution structure of the C-terminal domain of human p63 (505-579) was solved through NMR spectroscopy (54). The resulting structure shows a monomer with the characteristic five-helix bundle topology observed in other SAM domains (38). It includes five tightly packed helices with an extended hydrophobic core to form a globular and compact structure (54), helix 1 (α1; residues 514–521), helix 2 (α2; residues 527–533), a short 3^{10} helix (H3; residues 538–542), helix 4 (α4; residues 546–551), and helix 5 (α5; residues 556–573). A short and distinct β-sheet brings together the N-terminus and the third 3^{10} helix and the two antiparallel helices 1 and 5 form the hydrophobic core with the other three helices (Fig. 3).

A sequence alignment of p63- and p73-like SAM domains in different organisms highlights the importance of several residues. The aliphatic isoleucine and leucine residues (I549, L553, L556, I573, I576, L584, L587, I589, I597 and I601) that are part of a compact hydrophobic core are highly conserved in all SAM domains. G557 is also conserved suggesting an important role in forming a turn before the C-X-X-C motif. Interestingly, this sequence is not always present and can be replaced by an L-Q / G-A-Y motif. Several surface-exposed aspartates, lysines, arginines and serines are also highly conserved. The two highly conserved residues F552 and F565 participate in the formation of the hydrophobic core. F593 is partially solvent exposed and can be substituted for either histidine or tyrosine in other SAM domains. The fully conserved tryptophan at position 598 in both p63α and p73α SAM is solvent exposed, whereas in homologous SAM domains it participates in hydrophobic core formation. Most of the conserved hydrophobic residues appear to be involved in stabilizing the fold, although some of the solvent-exposed residues may have a functional role. The p63α SAM domain differs from p73α by

containing a free cysteine (C547) instead of a proline, possibly helping in the formation of a small β-sheet region, and the C-terminus of p63α SAM is significantly longer (55).
Unlike the other SAM domains neither p63 nor p73 SAM domains are able to form homodimers through their SAM domain. One possibility is that the SAM domains of p63 and p73 interact with the SAM domain of other proteins or with proteins that do not have a SAM domain at all (46).
Very little is known about the function of the SAM domain in p63 and very few interactors have been discovered, such as ABBP1 (apobec-1-binding protein-1) and Scaf4/rA4 (56) or Cables1 (cyclin-dependent kinase (Cdk) 5 and Abl enzyme substrate 1) (57).
Both ABBP1 and Scaf4/rA4 are RNA-binding proteins that function in RNA processing and play a critical role in mRNA splicing. These proteins are involved in several RNA-related biological processes such as transcription, pre-mRNA processing, mRNA export from the nucleus to the cytoplasm, and mRNA translation. However, the major role of the hnRNP proteins is regulation of mRNA splicing. The physical interaction between ABBP1 and the SAM domain of p63 led to a specific shift of FGFR-2 (fibroblast growth factor receptors-2) alternative splicing toward the K-SAM isoform essential for epithelial differentiation. AEC mutants completely abolished this interaction thus leading to the inhibition of epithelial differentiation and accounts for the AEC phenotype (56).
Cables1, a Cdk-interacting protein, protects p63 from ubiquitin-mediated proteasomal degradation through direct physical interaction with the TA and SAM domains of TAp63α and with ΔNp63α. Cables1 stabilizes p63α by blocking ubiquitin-mediated proteasomal degradation of the protein. This process is required for maximal stabilization of TAp63α in female germ cells, and the subsequent death of these cells, after exposure to a genotoxic stress in vivo (57).

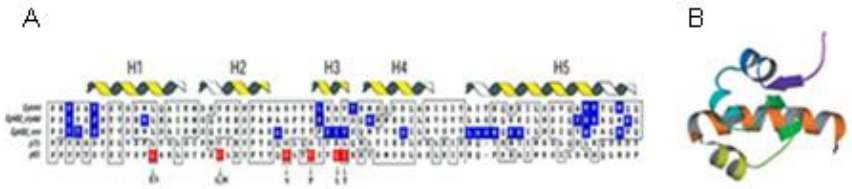

Figure 3: SAM domain. (A) Multiple sequence alignment of SAM domains of p63 with SAM domains of other proteins. The five helices are indicated as H1–H5. The white helices are the helices in the Eph receptors and the yellow parts are the helices in p73. Identical and similar amino acids are depicted in white boxes. Residues that are involved in dimerization are highlighted in blue. The mutated amino acids in p63 are indicated with red boxes (Adapted from McGrath et al, Hay-Wells syndrome is caused by heterozygous missense mutations in the SAM domain of p63, Hum Mol Genet, 2001). (B) The crystal structure of p63α SAM domain (Adapted from Sathyamurthy et al., Structural basis of p63a SAM domain mutants involved in AEC syndrome, The FEBS Journal, 2011)

- PS domain, also known as Trans-Inhibitory domain:

The PS domain, located after the SAM domain, has about its same length and shows no homology to any known sequence, aside from the equivalent region of p73α.

It is encoded by exon 14 of p63 and can be divided in two subdomains: the N-terminal subdomain (the first 45 amino acids) can bind and mask the TA domain of the p63 protein blocking its transactivation function. For this reason this PS domain is also called Trans-Inhibitory Domain (TID). The C-terminal subdomain (the last 25 amino acids) contains a sumoylation site that is involved in the regulation of the p63 protein degradation (58- Fig. 4).

The NMR studies of the PS domain has shown that this domain lacks secondary structure, as characterized by a narrow range of proton chemical shifts (24).

To further understand the role of this domain experiments of GST pull down assay have been made with PS domain in the context of TA and ΔNp63 isoforms. The results obtained showed that PS domain

strongly interacts with three hydrophobic residues of the TA domain F16 W20 and L23, conserved in all p53 family and known as MDM2 binding site (24). This intramolecular interaction obviously involves TAp63α that contains both TA and PS domain and forms a closed and inactive conformation of the trascription factor. The PS domain of ΔNp63α cannot interact intramolecularly since it lacks its own TA domain. However, p63 tetramerizes (59), and formation of hetero-oligomers between TAp63γ, the most active isoform, and ΔNp63α could allow PS domain to interact with the TA domain of another protein within the tetramer, acting in a dominant-negative manner (24).

Moreover, to demonstrate the inhibitor function of this domain, transactivation assay of different p63 isoforms and PS deleted mutants have been made and showed that the PS domain is both necessary and sufficient for inhibiting the activity of p63 (24).

Using a similar approach and alanine scanning studies, Straub et al. (57) have identified among the amino-acids 605 to 616, highly conserved from different species, a core domain responsible for the intramolecular interaction with the TA domain, in particular the residues FTL (605-607) and TIS (610-612).

It is known that a S/TQ phosphorylation site, present in the SAM domain may trigger a conformational change required for dismantling TAp63α intramolecular interaction between the TA and PS domains to render the normally transactivation inhibited TAp63α isoform more transactivation-competent, as described in oocytes (60).

Finally, after induction of apoptosis, the PS domain of the p63α isoforms is cleaved at a single site, amino-acid 458, by activated caspases -3. Cleavage of ΔNp63α relieves its inhibitory effect on the transcriptionally active p63 proteins, and the cleavage of TAp63α results in production of a TAp63 protein with enhanced transcriptional activity. So, the results of this cleavage is an increased transcriptional activity on proapoptotic genes and in general in an increased cellular apoptosis (61).

About the last 25 amino-acids of the PS domain it is known the presence of a sumoylation site IKEE (K637) targeting by SUMO-1 and SUMO-2 (Small Ubiquitin-like Modifier 1 and 2) (62), also highly conserved in vertebrate sequences. Surprisingly, however, the sumoylation site is missing in invertebrate ones. Further sequence

analysis revealed an (I/V)KEE sequence N-terminal to the SAM domain in all sequences that miss the C-terminal sumoylation site. Investigation of the corresponding TAp63α protein of Mytilus trossulus (mt-TAp63α) suggested that the elements that control the transcriptional activity in mammalian TAp63α are indeed conserved in this invertebrate protein (57). Sumoylation can have different effects on proteins and can influence stabilization, destabilization, or intracellular localization (63-67). In the case of p63, sumoylation has been reported to destabilize the protein (62). It does not seem to be directly involved in suppressing the intrinsic transcriptional activity of p63, but acts indirectly by controlling the intracellular level.

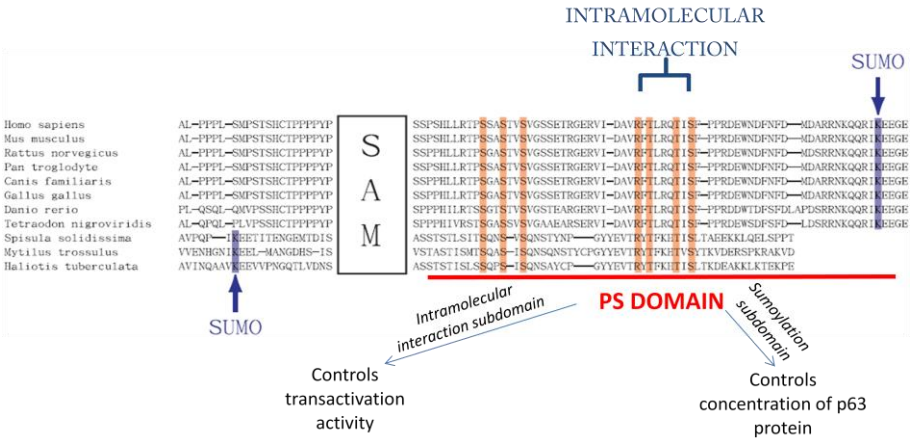

Figure 4: PS domain. Sequence alignment of C-terminal p63 sequences of various vertebrate and invertebrate species. Sequences N-terminal to the SAM domain to the end of the protein are shown. The sequences of the SAM domains themselves are not shown. Strictly conserved amino acids are labeled red. The conserved KEE sumoylation motif is labeled in blue. This sumoylation sequence is located N-terminal to the SAM domain in invertebrate species. (Adapted from Straub et al., The C-terminus of p63 contains multiple regulatory elements with different functions, Cell Death and Disease, 2010)

1.4 p63-deficient mice

In the 1999, two independent groups obtained a p63-deficient mouse models. Using these models they could explore the unique roles of p63 in development of ectodermal derived tissues.
$p63^{-/-}$ mice die for dehydration shortly after birth and display cleft palate, limb truncation and absence of all stratified epithelia, including the epidermis (9, 10), suggesting that p63 plays a non-redundant role in these tissues. p63-deficient newborns show striking limb defects (Fig. 5A). The forelimbs were truncated and hindlimbs were completely absent. Phalanges and carpals were absent in all of the p63-homozygous mutant, whereas more proximal forelimb structures were slightly heterogeneous in the extent of the truncation. The femur and all distal skeletal elements were also absent. These defects are caused by a failure of the apical ectodermal ridge (AER) to differentiate. During embryogenesis, the apical ectodermal ridge, a structure required for limb outgrowth along the proximal-distal axis, can be seen in the scanning electron micrograph at the junction of the dorsal and ventral surfaces of the distal tip of the limbs of E11.5 wild-type embryos. In contrast, the limb buds of p63-deficient embryos are distinctly smaller and misshapen, and there is no morphologically distinct AER. Several genes that are important in limb-bud outgrowth are not expressed, such as Fgfr8 (a marker of the AER) and Msx-1 (which expression in the mesenchyme depends on an ectodermal signal), or abnormally expressed, such as Lmx-1 (a marker of the dorsal limb mesenchyme) (9). Their skin does not progress past an early developmental stage: it lacks stratification and does not express differentiation markers. The surface of p63-deficient skin is covered by a single layer of flattened cells, without the spinosum, granulosum and stratum corneum (Fig. 5B). Structures dependent upon epidermal-mesenchymal interactions during embryonic development, such as hair follicles, teeth and several glands, including mammary, salivary and lacrimal glands, are absent (9). Defects in the surface epithelium of p63-null mice have been ascribed to loss of proliferative potential of keratinocyte stem cells (68, 10), and/or altered epidermal stratification and cell differentiation associated with reduced expression levels of Krt5/Krt14, characteristic of the basal, or progenitor, cells of stratified squamous epithelium, and Krt1/Krt10, early markers of epidermal differentiation (11, 9, 69). In parallel with

suppression of epidermal keratins, loss of p63 results in aberrant expression of the simple epithelial keratins Krt8 and Krt18 both in vivo and in vitro (11, 33), suggesting that p63 may be involved in maintaining an epithelial gene expression program in mammalian cells. All these observations suggest that p63 has a crucial role in tissue morphogenesis and maintenance of epithelial stem cell compartment.

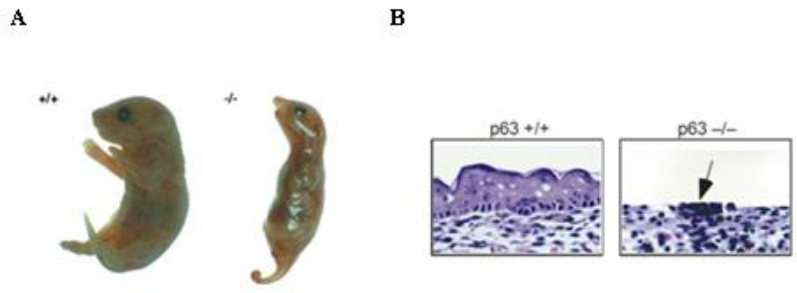

Figure 5: p63 knock-out mice. (A) The phenotype of p63-deficient newborn mice. Matings between p63-heterozygous mice produce wild-type and heterozygous offspring that are overtly normal and p63-deficient mice that have severe limb and skin defects. (Adapted from Mills et al., p63 is a p53 homologue required for limb and epidermal morphogenesis, Nature, 1999). (B) Defects in stratified epithelial differentiation in p63-deficient mice. Right, H&E stained sections of perinatal (E17-PI) $p63^{-/-}$ mice lacking squamous stratification in the epidermis; arrow shows cellular aggregates seen along the exposed dermis. Left, wild-type control H&E sections showing extensive stratification. (Adapted from Yang et al., p63 is essential for regenerative proliferation in limb, craniofacial and epithelial development, Nature, 1999)

1.5 p63-associated disorders

Heterozygous mutations in the transcription factor gene p63 are causative for several syndromes characterized by various combinations of ectodermal dysplasia (ED), orofacial clefting and limb malformations. Five different syndromes are already known: ectrodactyly, ectodermal dysplasia and cleft lip/palate syndrome (EEC, OMIM 604292), ankyloblepharon-ectodermal defects-cleft lip/palate syndrome (AEC, OMIM 106260), limb mammary syndrome (LMS, OMIM 603543), acro-dermato-ungual-lacrimal-tooth syndrome (ADULT, OMIM 103285) and Rapp- Hodgkin syndrome (RHS, OMIM 129400). Furthermore, two non-syndromic human disorders are caused by p63 mutations: isolated split hand/foot malformation (SHFM4, OMIM 605289) and recently non-syndromic cleft lip (NSCL). All p63-linked disorders are inherited in an autosomal dominant manner.

Ectodermal dysplasia manifests as the abnormal development or growth of tissue and structures that are developed from the outer embryonal layer, ectoderm. Skin, hair, teeth, nails and several exocrine glands, such as sweat and sebaceous glands are usually abnormally developed. The epidermis can be very dry and hypopigmented and with widespread erosed areas, in extreme cases. Hair is often diminished and can be wiry and curly, alopecia is sometimes reported. The teeth is often reduced in number and malformed, nails can be dystrophic, thickened and discoloured. Sweat glands are absent or reduced, the development and function of sebaceous and salivary glands are frequently abnormal, mammary glands and nipple are hypoplastic. There are also defects and obstruction of the lacrimal ducts.

The second main characteristic regards limbs. Hands and feet are often malformed and have severe median cleft in the palm and/or in the sole. Ectrodactyly, the lack of one or more central digits, and syndactyly, the fusion of fingers or toes, are present.

The third hallmark of p63 syndrome phenotype is orofacial clefting in the form of cleft lip (CL) and/or cleft palate (CP) (70).

EEC syndrome is characterized by one or more features of ectodermal dysplasia and an highly variability due to the exact nature of the causative mutation. EEC patients occasionally also have mammary gland/nipple hypoplasia (14%) and hypohidrosis (11%).

About two-thirds of these patients have ectrodactyly, and syndactyly is also frequent (43%). Cleft lip/palate is present in about 40% of the EEC patients, mostly as CL with or without CP (71).
EEC is mainly caused by point mutations in the DNA binding domain (DBD) of the p63 gene. Altogether 34 different mutations have been reported, and 20 different amino acids are involved. Only two mutations are outside the DNA binding domain: one insertion (1572 InsA) and one point mutation (L563P) in the sterile a motif domain (SAM) (72, 71). The EEC DNA binding domain mutations appear to impair the p63 protein binding to DNA.
AEC syndrome phenotype differs from the other conditions mainly by the severity of the skin phenotype, the occurrence of an eyelid fusion at birth and the absence of limb malformations. Approximately 80% of the patients have severe skin erosion at birth, which usually will recover in the first years of the life. The eyelid fusion, also called ankyloblepharon, is present in about 45% of AEC patients. Nail and teeth defects are present in more than 80% of patients, and hair defects and/or alopecia are almost constant features (94%). Lacrimal duct obstruction is seen in 50% of patients, whereas mammary gland hypoplasia and hypohydrosis occur occasionally (both 13%). Interestingly, almost 40% of patients have hearing impairment and genito-urinary defects. Cleft lip is present in 44% and cleft palate in about 80% of cases. Limb malformations are almost absent. Ectrodactyly has never been reported, but 25% of patients has only mild syndactyly (71).
RHS mimics AEC very much, the differences are the absence of ankyloblepharon in RHS and the more severe skin phenotype in AEC. The strong overlap between AEC and RHS suggest that they are variable manifestations of the same clinical entity (71, 73). AEC and RHS mutations are located in the C-terminus of the p63 protein. They are either point mutations in the SAM domain or deletions in the SAM or PS domains (46, 47, 72, 74-82).
EEC and AEC/RHS syndromes are good examples of a strong genotype – phenotype association.
A consistent feature of **LMS** is the mammary gland and/or nipple hypoplasia (100%). Lacrimal duct obstruction and dystrophic nails are frequently observed (59 and 46% respectively), hypohydrosis and teeth defects are detected in about 30%, but other ectodermal defects such as hair and skin defects are rarely detected if at all. About 70% of

LMS patients have similar limb malformations as in EEC syndrome, and about 30% orofacial clefting, notably always in form of cleft palate (74). Mutations in LMS are located in the N- and C-terminus of the p63 gene.

About **ADULT syndrome**, teeth, skin, nail, hair and lacrimal duct defects are constantly present in ADULT syndrome (100, 91, 100%, 53% and 67%, respectively). A point mutation in exon 8, changing R298 in the DNA binding domain into either a glutamine or a glycine has been found. While EEC syndrome mutations in the DNA binding domain impair the binding of p63 protein to DNA (72), arginine 298 is not located close to the DNA-binding interface, and mutation of this arginine does not affect DNA binding (83). Two other mutations are located in the N-terminus.

SHFM4 is a "pure" limb malformation (ectrodactyly and syndactyly) condition, thus without orofacial clefting or ectodermal dysplasia. It is caused by several mutations, which are dispersed throughout the p63 gene. Possibly, SHFM is caused by altered protein degradation, even though different degradation routes are involved (70).

A **non-syndromic orofacial clefting type** was also linked to p63 gene, R313G is the first mutation discovered (84).

Several examples show that the same mutation can lead to different clinical conditions. The possible explanation is the influence of cis-acting polymorphisms and/or the effects of modifier genes. The phenotypic variation between the *p63*-linked diseases is large, furthermore the phenotypic variation within one disease is also considerable. It is clear that variability within families may be ascribed to a combination of modifier genes, and stochastic processes (70 - Fig. 6).

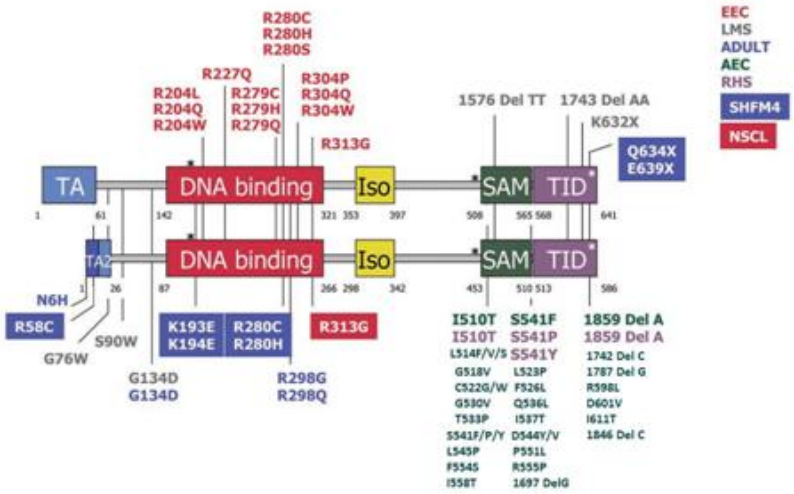

Figure 6: p63 and its mutations. Pathogenic p63 mutations cause at least five different syndromes and two non-syndromic conditions. Mutations causing different diseases are illustrated in different colours. EEC hotspot mutations are clustered in DNA binding domain, and RHS and AEC syndrome mutations in SAM and PS domains. Several mutations, such as R280, R313, I510, S541 and 1850 Del A, can have a variable clinical outcome, probably due to genetic background effects. The black asterisks illustrate sites needed for upiquitination (K193, K194 and PY) and the white asterisk represents a sumoylation site (fKXD/E). TA= Transactivation domain; Iso= oligomerization domain; SAM= Steril alpha Motif; TID= Post-SAM domain. (Adapted from Rinne et al., p63-Associated Disorders, Cell Cycle, 2007)

1.6 AEC syndrome

About 10% of p63-linked patients have AEC. This syndrome, also known as Hay–Wells syndrome, was first reported by Hay and Wells in 1976 (85). It is a rare autosomal dominant disorder characterized by congenital ectodermal dysplasia, including alopecia, scalp infections, dystrophic nails, hypodontia, ankyloblepharon and cleft lip and/or cleft palate (Fig. 7A-C).
Skin lesions are a distinctive signs of AEC syndrome. Adult patients can be affected by palmoplantar hyperkeratosis and erosive palmoplantar keratoderma with bleeding after extensive walking. The biological mechanisms underlying the skin erosions remain unveiled, and treatment is limited to gentle wound care and antibiotic treatment to prevent or cure infections. Healing is slow and recurrent breakdown is typical.
AEC syndrome causative mutations mainly fall in the C-terminus of p63 protein and include twenty-five missense and only two frameshift mutations in the SAM domain, whilst in the PS domain predominate the frameshift mutations that extend p63 protein. Recently, novel AEC causative mutations have been identified that result in translation re-initiation downstream of the non-canonical transactivation domain in the ΔN-specific isoforms, leading to expression of truncated ΔNp63 protein with dominant negative effects (86).
The mutations best characterized involve the SAM domain and can be separated in two different group. The first subgroup contains those mutations that affect amino acids that are predicted to be buried inside the protein and have a small solvent accessible surface. The second subgroup contains all other amino acids that have a larger solvent accessible surface. Mutation of the first subgroup of amino acids is likely to affect the overall structure and stability of the protein by altering the packing of the helices (I549T, F552S, L553F, L553V, C561G, C561W, F565L, I576T, L584P and I597T). In contrast, the second subgroup of mutations is not predicted to cause gross conformational changes, but are clustered in a small region around helix 3, which could indicate that this region is involved in binding of the SAM domain to its interaction partner (G557V, G569V, T572P, Q575L, S580F, S580P, S580Y, D583C, D583Y, P590L, F593S, R594P, G600V and G600D).

To analyse the effect of these mutations, p63α SAM domain containing some of the point mutations above were cloned and expressed. The expression of point mutations found in the AEC syndrome varied significantly. The wild-type protein and the mutants L553V (L514V) and C561W were found to be over-expressed in the soluble fraction. In contrast, mutants L553F (L514F), C561G, G569V, Q575L and I576T were present only as inclusion bodies, but could be refolded easily during purification. The mutants G569V, Q575L and I576T partially aggregated at the gel filtration stage but sufficient material was purified to allow analysis. Compared with the wild-type, mutations L514F, C561G, C561W, G569V, Q575 and I576T are all significantly destabilized. A possible explanation for the instability of each of these point mutations was obtained by looking at the structural features of the wild-type protein. Mutation L514F, which is close to F552, would probably cause a severe steric clash between the two phenylalanine rings and result in overcrowding in the hydrophobic core. The tryptophan ring in C561W would possible result in a steric clash with the aromatic ring of F593. The instability of C561G is most probably caused by the formation of a hydrophobic cavity resulting from the loss of a bulky thiol group. The cavity created would potentially cause some rearrangement of the hydrophobic core and the associated instability. Introduction of a polar residue into the hydrophobic core, as happens with mutation I576T, would potentially lower the stability of the domain. Mutation G569V may cause instability due to the residues in the loops adopting a more unfavorable conformation. Mutation Q575L occurs in a solvent-exposed position and the side-chain carbonyl of Q575 forms a hydrogen bond with the main-chain amides of both T571 and T572. The side-chain hydroxyl of T572 forms an N-cap hydrogen bond with the main-chain amide of Q575 and thus a mutation to proline would abolish the potential to form this hydrogen bond. The location of the L514V mutation in the core of the domain precludes this being a functional mutation and hence the mutation also appears to be structural, possibly by creating a small hydrophobic cavity in the hydrophobic core. All the mutants are partially denatured or unfolded even under non-denaturing conditions. As such any attempt to crystallize the domains would be almost impossible (55). Mutations I549T and I597T would also introduce a polar residue into the

hydrophobic core, and presumably these mutants would be destabilized in a similar manner to mutation I576T. Mutations F552S and F565L would both result in the loss of a large aromatic residue from the hydrophobic core. Mutation G557V may cause instability due to the residues in the loops adopting a more unfavorable conformation in a similar manner to that observed for mutation G569V. Mutations S580F, S580P and S580Y would all result in the loss of the N-cap hydrogen bond from the main-chain amide of D583 to the side-chain hydroxyl of S580, whilst mutations D583C and D583Y would disrupt a hydrogen bond from the main-chain amide of S580 to the side-chain carbonyl oxygen of D583. Mutation R594P would disrupt a standard hydrogen bond in helix 5. Mutations G600V and G600D would probably result in a steric clash between α-helix 5 and L556. Finally, the in-frame 3 bp insert (573–574 inserting TTC) encoding an additional phenylalanine residue would be expected to be destabilizing as it probably disrupts the packing of the 3^{10}-helix to the rest of the protein. Of all the mutations only P590L and F593S could not easily be explained as mutations that would either disrupt the hydrophobic core or result in a loss of a stabilizing hydrogen bond or salt bridge. Indeed F593 is a solvent exposed aromatic residue and a mutation to a polar residue might even be expected to increase stability. Two mutations that appear not to be structural mutations, P590L and F593S, are close in sequence to two of the highly conserved hydrophilic residues (K588 and Q592) and may indicate that this interface plays some role in domain function (55- Fig. 6D).

Nothing is known about the mutations in the PS domain. Several explanations for the surprising absence of missense mutations in the core of the PS exist. First, such mutations could be lethal. Second, a syndrome would arise only if the mutations would create either a dominant-negative or a gain-of-function effect. If the main effect of mutations in the PS is a loss of the dominant-negative behavior toward other transcriptionally active forms, expression of the second, non-mutated allele might be enough to sustain the biological function of ΔNp63α during development and maintenance of epithelial tissue (58).

About the molecular mechanisms of action of these mutants little is known: generally the mutants are more stable than the wild-type protein and have a reduced transactivation capability (87).

To study the functional activity of mutant p63 in AEC syndrome a first knock-in mouse model ($p63^{+/L514F}$) was previously generated in our laboratory (88).

This model carries a phenylalanine substitution in position 514 (L514F) and closely resembles the human disease (88, 89). This mutation falls in the first helix of the SAM domain and disrupts the folding of the protein. Among the AEC causative mutations we decided to focus our attention on L514 amino acids for three reasons: first of all, this amino acid is mutated in three different amino acids (phenylalanine, valine or serine); this mutation affects an amino acid that is predicted to be buried inside the protein and has a small solvent accessible surface, so any mutation in this region is likely to affect the overall structure and stability of the protein by altering the packing of the helices, and moreover the substitution of a leucine with a phenylalanine probably cause a severe steric clash between two phenylalanine rings that are located close to each other (70, 46).

$p63^{+/L514F}$ mouse model is characterized by hypoplastic and fragile skin, ectodermal dysplasia and cleft palate. Ferone et al.,2010, found that epidermal hypoplasia and cleft palate are associated with a transient reduction in epithelial cell proliferation during development. These defects closely resemble those observed in the Fgfr2b-/- mice (90-94). Since p63 transcriptionally controls the Fibroblast growth factor receptors Fgfr2 and Fgfr3 and their expression, they found that impaired FGF signaling downstream of p63 is likely an important determinant of reduced ectodermal cell proliferation and defective self-renewing compartment in AEC syndrome.

Unfortunately, a neonatal lethality due to cleft palate prevented the generation of a mouse line and the studying of the adult phenotype (88).

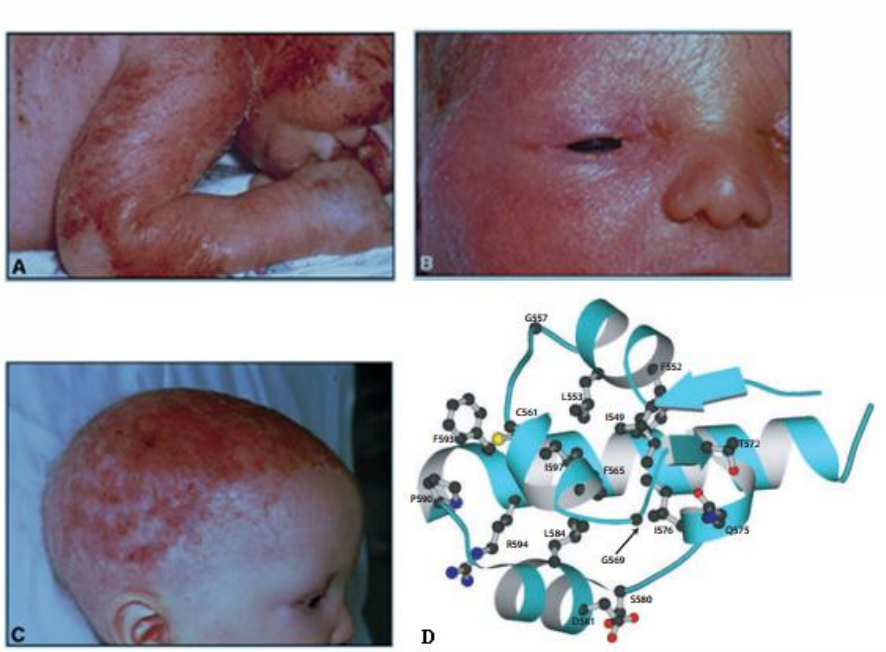

Figure 7: AEC phenotype and mutations. (A) A neonate with skin erytherma, erosions and cleft lip/palate. (B) A newborn with partial fusion of the eyelids(ankyloblepharon). (C) An 18-month-old child with extensive erosive scalp dermatitis and alopecia. (Adapted from McGrath et al., Hay-Wells syndrome is caused by heterozygous missense mutations in the SAM domain of p63, HMG, 2001). (D) Ribbon representation of the p63α SAM domain showing the position of mutations that are associated with AEC syndrome. (Adapted from Sathyamurthy et al., Structural basis of p63α SAM domain mutants involved in AEC syndrome, FEBS, 2011)

2. MATERIALS AND METHODS

2.1 Constructs and cell culures

AEC mutants were obtained using QuikChange site-directed mutagenesis (Stratagene) starting from pCMV2-FLAG mΔNp63α. All the constructs were achieved for PCR. To obtain E570fsX94 and N620fsX44, the mutagenesis to delete an aminoacid has been made after cloning in pCMV2-FLAG plasmid (Sigma) the N-terminal portion of human p63 from pcDNA3 plasmid (Not I-Nco I) together with a C-terminal portion of human p63 from cDNA of NHEK cells (Nco I-Bgl II). p63ΔSAM is obtained cloning the N-terminal (Not I-Sac II) and C-terminal (Sac II-Xba I) region of p63 without the portion corresponding to SAM domain without changing any aminoacid. Finally to obtain GFP N-terminal tagged ΔNp63α, p63 was removed from pCMV2-FLAG plasmid and inserted in pEGFP-1 using Bgl II.
HEK293 and COS7 cells were coltured in Dulbecco Modified Eagle Medium (Sigma) with 10% of Fetal Bovine Serum (FBS) and 2mM of Glutammine and incubated at 37°C, 5% CO2.
Primary mouse keratinocytes were isolated from skin of 2-day-old mice. They were placed in petri dishes with ice and inserted in an ice bucket. After 30-45' mice were washed twice with 70% ethanol and twice with water to remove ethanol completely. Using sterile techniques, mice tails and limbs were amputated with sterile surgical scissors. The skin was carefully separated from the rest of the viscera and flattened in a empty 150mm petri dish with the dermis facing down; 15 ml of Dispase solution (0.5mg Dispase-GIBCO, Na-bicarbonate 0.75%, Hepes 10mM, Antibiotic-Antimycotic in PBS) were added to each petri dish and incubated o/n at 4 °C. Next day epidermis was separated from the dermis and placed in a 100mm Petri dish in 2ml (for each epidermis) of 0.125% trypsin-2.5mM EDTA. Epidermis was minced with tweezers and scissors until is reduced in very small fragments and placed at 37°C for 5-8 minutes. Then trypsin is inactivated with DMEM+10% FBS and filtered using cell strainers in order to remove the floating particles. Cells were placed into the centrifuge for 5 minutes at 1000 rpm; then were plated on collagen

coated plates and incubated at 34°C, 8% CO2 in a Low Ca^{++} Medium (LCM) with the addition of 4% Chelex serum and EGF.

Oligonucleotide primers for mutagenesis and cloning:

E639X mutagenesi
CAGCGCATCAAAGAGTAGGGGGAGTGAGCC
GGCTCACTCCCCCTACTCTTTGATGCGCTG

Q634X mutagenesi
CGCCGCAATAAGCAATAGCGCATCAAAGAGGAG
CTCCTCTTTGATGCGCTATTGCTTATTGCGGCG

E570fsX94 and N620fsX44 cloning
CCCGGCGGCCGCGTTGTACCTGGAAAACAATGCCC
AGATCATCCATGGAGTAATGCTC
GAGCATTACTCCATGGATGATCT
GCGGAGATCTTCCCCTAAGAAATCAGACAAGAGG

E570fsX94 mutagenesi
CCGGCAGCTCCACGATTCTCCTCCCCTTCT
AGAAGGGGAGGAGAATCGTGGAGCTGCCGG

N620fsX44 mutagenesi
CCCCGAGATGAGTGGATGACTTCAACTTTGACATGG
CCATGTCAAAGTTGAAGTCATCCACTCATCTCGGGG

p63ΔSAM
AAGCTTGCGGCCGCGTTGTACCTGGAAAACAATGCC
AAGCTTCCGCGGGTAGGGCGGTGGTGGGGTGCAG
ACTTCCGCGGCAGCTGCACACGACTTCTCCTC
CCTCTAGATCATTCTCCTTCCTCTTTGATACGCTG

GFP-ΔNp63α
ACTTAGATCTTTGTACCTGGAAAACAATGCC
ACTTAGATCTTCATTCTCCTTCCTCTTTGATACG

2.2 Luciferase reporter assay (luc assay)

Subconfluent HEK293 cells in 12-well dishes were transfected using Lipofectamin 2000 (Invitrogen) at a 1:3 ratio between the reporter plasmid (containing the firefly luciferase gene under the control of K14 promoter) and the expression vectors encoding for wild-type and mutated ΔNp63α. 5 ng of Renilla Luciferase Vector (pRL-CMV; Promega) was co-transfected, as a control of transfection efficiency. At 24 h after transfection, cells were washed twice with PBS and luciferase activities of cellular extracts were measured, by using a Dual Luciferase Reporter Assay System (Promega); light emission was measured using a luminometer. Efficiency of transfection was normalised using Renilla luciferase activity.

2.3 Western Blot (WB)

Cells were lysed in sample buffer (10% glycerol, 0.01 % Bromophenol Blue, 0.0625 M Tris-HCl pH 6.8, 3 % SDS, 5 % ßmercaptoethanol). Extracts were run on SDS-PAGE gels, transfer on Immobilon-P transfer membranes (Millipore), probed with the indicated antibodies and detected by chemiluminescence (ECL, GE Healthcare Life Sciences). The following primary antibodies were used for immunoblotting analysis: p63 (4A4, 1:200), β–actin (1:1000) and ERK-1 (1:5000), provided by Santa Cruz Biotechnology.

2.4 Co-Immunoprecipitation (Co-IP)

HEK293 and COS7 were plated on 60mm plates and transfected with Lipofectamine 2000 and 4mg of wild-type and mutated FLAG and GFP-DNp63a. After 48 hours, cell were washed twice with PBS and lysed in 600mL of Busslinger lysis buffer (20mM Tris-HCl pH7.9, 120mM KCl, 5mM MgCl2, 0.2mM EDTA pH8.0, 0.2% NP40, 10% Glycerol) with the addition of protease and phosphatase inhibitor and dithiothreitol for 15 minutes on ice. After scraping and discard the pellet, the total amount of proteins were measured with Bradford protein assay and normalized among different samples. 10mL of anti-FLAG M2 (50% slurry) conjugated agarose beads (Sigma) were used to immunoprecipitate for 2 hours at 4°C. Resin was washed 4-5 times

with Busslinger lysis buffer with the addition of dithiothreitol and Phenylmethanesulfonyl fluoride and finally resuspended in sample buffer at 65°C. Part of total extract and immunoprecipitates were analyzed by western blotting.

2.5 Protein Expression and Purification in E. coli and Size Exclusion Chromatography (SEC)

Genes for murine TAp63a and ΔNp63α were cloned into pMAL-c4X vector (New England Biolabs, NEB). All proteins had an additional C-terminal and/or N-terminal His6-tag. Proteins were expressed in T7 express competent E. coli cells (NEB) and purified using Ni-Sepharose Fast Flow (GE Healthcare) and Amylose resin (NEB) according to standard protocols. Proteins were further purified by size exclusion chromatography (SEC) using a preparative Superose 6 column (GE Healthcare) in 10 mM potassium phosphate buffer (pH 7.6) with 200 mM NaCl. All following experiments were performed in this storage buffer if not denoted differently.
SEC of recombinant proteins expressed in E. coli was performed at 16° C using a Superose 6 10/300 GL column (GE Healthcare), calibrated using Blue Dextran 2000, Thyroglobulin (669 kDa), Ferritin (440 kDa), Aldolase (158 kDa), and Ovalbumin (43 kDa) (GE Healthcare).

2.6 Chromatin Immunoprecipitation (ChIP)

1 x 10^6 mouse keratinocytes and 5 x 10^6 HEK293 cells were fixed with 1% formaldehyde in growth medium at 37°C for 10 min. Extracts were sonicated using BIORUPTOR (Diagenode) to obtain DNA fragments ranging from 400 to 800 bp in length. Chromatin was immunoprecipitated as in the Upstate protocol (http://www.upstate.com). Immunoprecipitation was performed using anti-p63 (H-137; Santa Cruz Biotechnology) and anti-ERK-1 (K23; Santa Cruz Biotechnology) antibodies as negative control. Real-time PCR was performed using the SYBR Green PCR master mix in an ABI PRISM 7500 (Applied Biosystems).
About ChIP *in vivo* isolate skin from E14.5 embryos were fixed with 1% formaldehyde, rotated 15 minutes at room temperature and

blocked with glycine. The obtained cells pellet was treated as described above.

Oligonucleotide primers used for ChIP

human CST8H (97)
CGTTCCAAAGCCTAACCTGATCA
TTTTCCCAAACTCCAACCTG

human Fgfr2Int1 (88)
CCCCGTGGCCGAAAA
GAAAGCGCAGGCGAGTTCT

human K14prom/enh
GGGCCTGTCTGAGGAGATAGG
AGGCATGTTGAGAGGAATGTGA

mouse CST8H (97)
CTGCGTGTGCGTTGCATATAA
CGTCATGTCTCCCTGCCTTC

2.7 Preparation of nuclear extracts and Electrophoretic Mobility Shift Assay (EMSA)

To prepare nuclear extracts, cells were scraped from dishes into isotonic cold phosphate-buffered saline and collected by centrifugation at 1,850 ×*g* for 10 minutes. The pellet was resuspended in 5×volume of buffer A (10mM HEPES pH 7.9, 1.5mM $MgCl_2$, 10mM KCl, 1mM dithiothreitol, and freshly added protease inhibitors). Cells were incubated on ice for 10 minutes and centrifuged at 1,850 ×*g* for 10 minutes. The pellet was resuspended in 2×volume of buffer A and homogenized using Dounce Homogenizer (10–15 strokes). Nuclei were pelleted by centrifuging for 2 minutes at 12,000 ×*g*. Nuclei were resuspended in 2×volume of high-salt buffer B (20 mM HEPES, 25% glycerol, 1.5mM $MgCl_2$, 0.45M NaCl, 0.2mM EDTA, 1mM dithiothreitol, and freshly added protease inhibitors) and rotated end on end on a Rota-Mixer for 30 minutes at 4°C. Nuclear extracts were collected from the supernatant by centrifugation in a microcentrifuge at 13,500 ×*g* for 30 minutes, flash frozen, and stored at -80°C.

For EMSAs, complementary oligonucleotides spanning the regions of interest were synthesized (IDT Technologies), annealed, and 2pm of double-stranded oligonucleotides was used for radioactive labeling with [α-^{32}P]dCTP. A 1–3 bps 5' overhang was designed at each end to allow labeling by fill-in with Klenow polymerase. After labeling, probes were purified using G-50 Nick columns (Amersham, Piscataway, NJ). Binding reactions were performed at room temperature in 20μL of DNA-binding buffer (20mM HEPES, pH 7.9, 75mM KCl, 10% glycerol, 1mM dithiothreitol, and 2.5mM $MgCl_2$) with 4–6 μg of nuclear extracts. One microgram of poly(dA-dT) or poly(dI-dC) was added as a nonspecific DNA competitor. For supershift assays, antibodies were preincubated with nuclear extracts for 20 minutes at room temperature before addition of labeled probe. Antibody used in EMSAs was anti-p63 (RR-14). The protein–DNA complexes were resolved by gel electrophoresis on 5% non-denaturing polyacrylamide gels at room temperature. Gels were dried and visualized by autoradiography.

Oligonucleotide primer used for EMSA

K14 enhancer site (101)
GCAGGGGCTGTTGGGGCCTGTCTGAGGA

2.8 Generation of a conditional AEC mouse model

Neonatal lethality in heterozygous p63$^{+/L514F}$ (88) prevented the generation of a mouse line and the studying of the adult phenotype. To overcome lethality, we recently generated a conditional knock-in model (p63$^{+/floxL514F}$), in which the L514F mutation is inserted in exon 13 and expressed only in the presence of the Cre recombinase. A 3xFLAG tag was inserted at the C-terminus of the mutant protein. The construct was inserted by recombination in murine embryonic stem (ES) cells. A neomycin cassette was inserted to select positive clones of ES cells and it can be removed by Flp-mediated recombination.

2.9 Mouse genotyping

Conditional knock-in $p63^{+/L514F,L514F/L514F}$, knock-in $p63^{+/L514F}$ and $p63^{+/-}$ mutant mice were genotyped by PCR using genomic DNA isolated from mouse tails.

Oligonucletide primers used for PCR

Conditional knock-in $p63^{+/L514F,L514F/L514F}$
CAGCGTATCAAAGAGGAAGGAGA
AGCCAGAATCAGAATCAGGTGAC
The expected bands were of 250bp for the wild-type mice, 337bp for the mutant homozigous mice and both for the heterozigous ones.

knock-in $p63^{+/L514F}$ (88)
GTCTGACCTCCCGACCCACCTCCT
GCATGATGAGCAGCCCAACCTTGCT
GCATGATGAGCAGCCCAACCTTGCA
The first was the forward primer in common for the amplification of wild-type and mutant allele, while the reverse primer differed only at 3' for the presence of the point mutation. Genomic DNA from $p63^{+/L514F}$ was amplified by both couples of primers, whereas genomic DNA from wildtype littermates was amplified only by the oligo reverse with the correct base in 3' first position.

$p63^{+/-}$ (102)
GTGTTGGCAAGGATTCTGAGACC
GGAAGACAATAGCAGGCATGCTG
The wild-type mice had no bands, while for the heterozigous ones the band expected was of 450bp.

2.10 Adenovirus infection

Mouse primary keratinocytes were infected after 4-5 days of plating, when they reached confluence. Adenovirus carring the GFP or the Cre-recombinase (provided by OKAIROS) at MOI 100 were diluted in 200μL and 1.2mL respectively for 12-well and 60mm

dishes of LCM without serum and EGF. After 2 hours of infection, supplemented medium was added and left o/n at 34°C.

2.11 RT real time PCR

Total RNA was extracted two and four days after infection from primary keratinocytes using TRIzol reagent (Invitrogen). cDNA was synthesized using SuperScript Vilo (Invitrogen). Two-step real-time reverse transcription RT-PCR was performed using the SYBR Green PCR master mix in an ABI PRISM 7500 (Applied Biosystems). Levels of the target genes were quantified using specific oligonucleotide primers and normalized for Actb (β-actin) expression.

Oligonucletide primers used for Real-Time RT-PCR

mouse Actin
CTAAGGCCAACCGTGAAAAGAT
GCCTGGATGGCTACGTACATG

mouse Krt5
CAACGTCAAGAAGCAGTGTGC
TTGCTCAGCTTCAGCAATGG

mouse Krt14
ACCACGAGGAGGAAATGGC
TGACGTCTCCACCCACCTG

mouse Dsc3
CCACCGTCTCTCACTACATGGA
TGTCCTGAACTTTCATTATCAGTTTGT

mouse Dsp
CACCGTCAACGACCAGAACTC
GATGGTGTTCTGATTCTGATGTCTAGA

mouse IRF6
CAGCTCTCTCCCCATGACTGA
CCCATACTCCTTCCCACGATAC

mouse Fgfr2
TGGATCGAATTCTGACTCTCACA
TTCGAGAGGCTGGGTGAGAT

2.12 Histopathology

E18.5 embryos were dissected, fixed overnight in 4% paraformaldehyde (PFA) and embedded in paraffin using standard methods. Sections (7 μm) were deparaffinized and stained with Haematoxylin and Eosin (H&E) . The pictures of skin were taken using a Zeiss Axioskop2 plus Microscope.

3. RESULTS

3.1 AEC mutants have an impaired ability to induce p63 target genes

To explore the mechanism underlying AEC syndrome we tested the possibility that AEC mutant proteins may have an impaired ability to activate transcription of p63 target genes. For this reason we tested a number of p63 mutants characteristic of AEC syndrome in transactivation assay in heterologous cells.

Specifically we analyzed the transcription activation of missense mutations involving the SAM domain, L514F, G534V (46), C519R, D544Y, and frameshift mutations in the PS domain, E570fsX94 (76) and N620fsX44 (70), that extend p63 protein of 94 and 44 amino acids respectively. In addition we also tested an EEC mutation, R304Q (75), and two SHFM mutations, Q630X (95) and E635X (74). A luciferase reporter assay was performed in p63-null HEK293T cells as described (94) using the firefly luciferase gene under the control of the Krt14 promoter, which modulates the expression of a protein physiologically expressed in basal keratinocytes. As reported by Serra et al., 2011 (95), the mutation that disrupt the DNA binding domain, displayed a reduced activity (here we used R304Q), while the mutations causative of SHFM, Q630X and E635X, displayed a transcriptional activity similar to wild-type protein, as expected since Krt14 is not involved in this pathogenesis. We found that missense mutations of SAM domain and frameshift mutations of PS domain displayed a very strong reduction of transcriptional activity. Interestingly, this reduction was stronger than that observed for the DBD mutation (Fig. 8A).

To further explore the role of the two C-terminal domains of p63α isoform, that are involved in AEC syndrome, we obtained two deletion p63 mutants that lack alternatively SAM (p63ΔSAM) or PS (p63ΔPS) domain, and tested their transcriptional activity on Krt14 promoter. We found that p63ΔSAM had a reduced capability to transactivate, whilst p63ΔPS had a stronger activity than the wild-type ΔNp63α protein (Fig. 8B).

These results demonstrate that all AEC causative mutations have an impairment to activate the transcription of p63 target genes, moreover

lack of the SAM domain also impaired p63 activity while lack of PS domain does not.

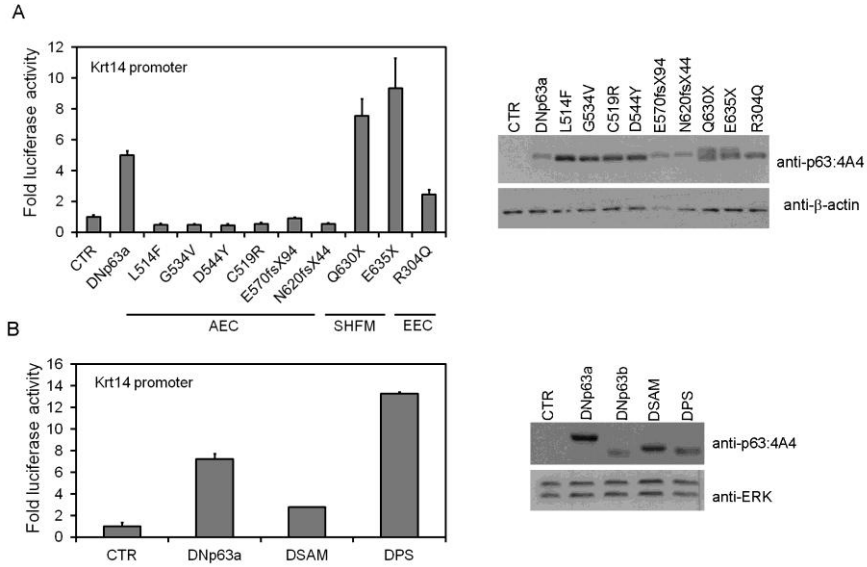

Figure 8: AEC p63 mutants and DSAM do not activate transcription. (A) Luc assay on Krt14 promoter region in HEK293T cells reveals that ΔNp63α, Q630X and E635X can activate transcription but not AEC mutants, L514F, G534V,D544Y, C519R, E570fsX94, N620fsX44. EEC mutant R304Q is used as negative control of transactivation. The picture is representative of three independent experiments. On the right side of picture western blot analysis of p63 mutants revealed with anti-p63 4A4 antobodies and normalized for β-actin. EEC= ectrodactyly, ectodermal dysplasia and cleft lip/palate syndrome; AEC= ankyloblepharon-ectodermal defects-cleft lip/palate syndrome; SHFM= split hand/foot malformation. (B) Luc assay on Krt14 promoter region in 293T cells reveals p63ΔSAM, but not p63ΔPS, has an impairment in activate transcription. The picture is representative of four independent experiments. On the right side of picture western blot analysis of p63 deletion mutants revealed with anti-p63 4A4 antobodies and normalized for total ERK. DSAM= p63ΔSAM; ΔPS= p63ΔPS; CTR= negative control.

3.2 AEC mutations do not affect tetramerization

In mouse oocytes TAp63α exists in a closed dimeric conformation and phosphorylation triggers the formation of active TAp63α tetramers. This switch from dimers to tetramers increases the DNA binding affinity of p63 of about 20 fold. In contrast, the most abundantly expressed isoform in the skin, ΔNp63α, forms tetramers, since it lacks the TA domain (96).

Since AEC mutants have lost the ability to transactivate transcription, we asked if the reason is the inability to tetramerize with themselves and with wild-type proteins. First of all, we performed Co-IP assays both in HEK293FT and in COS7 cells. To this purpose, we tagged the various p63 protein with either GFP or FLAG, and we transfected them in different combination. Western blot analysis of the immunoprecipitates displayed that in all different combinations the L514F mutant protein is able to bind wild-type protein and itself (Fig. 9A).

Co-IP assays were also performed with ΔNp63α proteins lacking the SAM and PS domains. FLAG deleted mutants were co-transfected with GFP wild-type protein and, as expected, both mutants are able to bind wild-type counterpart (Fig. 9B).

In collaboration with Prof Volker Dötsch (Institute of Biophysical Chemistry and Center for Biomolecular Magnetic Resonance, Goethe University, Frankfurt 60438, Germany), we performed a size exclusion chromatography (SEC) analysis of purified murine L514F mutant p63 protein expressed in Escherichia coli. The classification of p63 as a dimer or tetramer was based on a calibration of the SEC column with compact globular proteins. An enrichment at a SEC elution fractions 1.30 ml correspond to an elution of a tetrameric protein, while an elution at 1.55 ml correspond to a dimeric protein. TAp63αL514F, similarly the wild-type, eluted as a dimeric protein, while ΔNp63αL514F eluted as a tetramer, as its wild-type counterpart (96- Fig. 9C).

These results indicate that L514F p63 mutant is able to associate with wild-type ΔNp63α protein and itself, and retains the ability to tetramerize. Moreover p63ΔSAM and ΔPS are able to bind wild-type ΔNp63α protein, indicating that these two C-terminal domains are not involved in homodimerization of ΔNp63α.

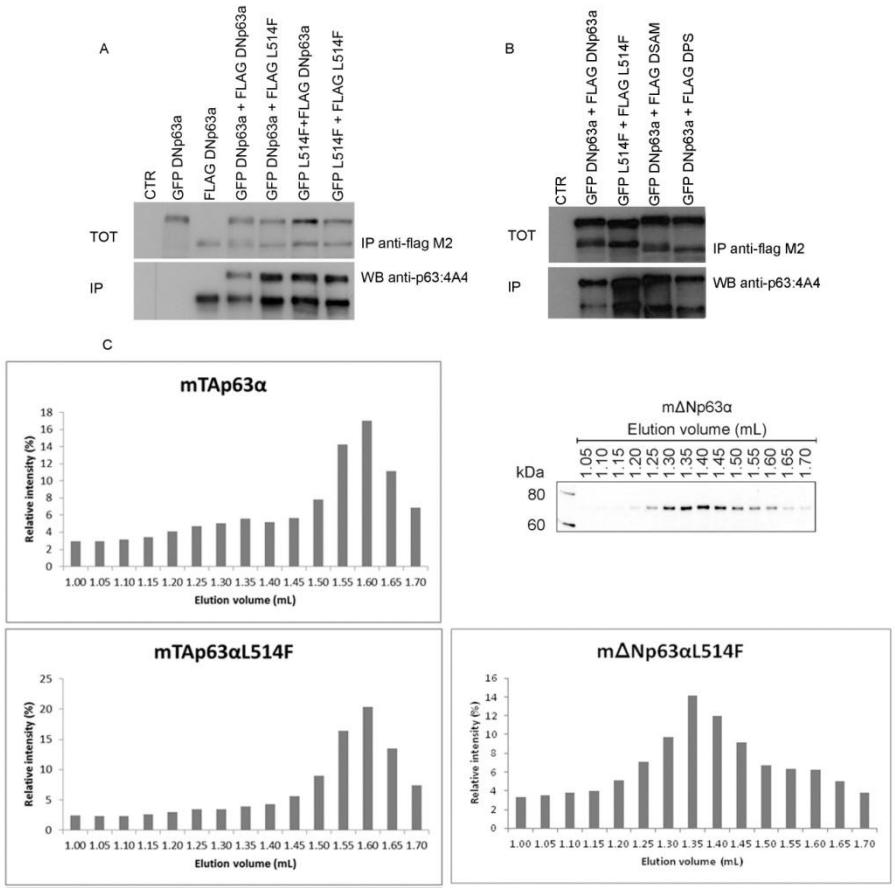

Figure 9: AEC L514F p63 mutant is still competent to tetramerization. (A) Co-IP assay with GFP or FLAG tagged wild-type ΔNp63α and AEC L514F mutant transfected in HEK293FT cells in different combination reveals that AEC mutant is able to dimerize with wild-type protein and itself. GFP- ΔNp63α and FLAG- ΔNp63α is used as control of Co-IP. Part of total extract and immunoprecipitates were analyzed by western blotting. (B) Co-IP assay in HEK293FT cells revealed that p63ΔSAM and p63ΔPS are able to dimerize with wid-type ΔNp63α. TOT= total; IP= immunoprecipitates; WB= western blot; DSAM= p63ΔSAM; ΔPS= p63ΔPS; CTR= negative control. (C) Bar diagram showing relative p63 signal intensities of SEC elution fractions from 1.00 to 1.70 ml of

mTAp63α, mTAp63αL514F and ΔNp63αL514F, and western blot of SEC elution fraction from 1.05 to 1.70 ml of ΔNp63α. The enrichment is at 1.55 for mTAp63α and mTAp63αL514F indicating their dimeric elution, and at 1.30 for ΔNp63α and ΔNp63αL514F indicating their tetrameric elution. m= mouse.

3.3 AEC mutant proteins bind DNA less efficiently than wild-type p63

To test the hypothesis that AEC mutants may be unable to transactivate p63 target genes due to an impaired ability to bind DNA, we performed ChIP assays in HEK293FT cells with an anti-p63 antibodies (H137). We transfected ΔNp63α and L514F p63 mutant alone or in combination and analyzed DNA binding to different p63 genes, such as p63 itself in the C40 (97) enhancer element and Fgfr2 (88). The DNA binding p63 mutant R304Q was used as negative control. In both binding regions we found that L514F p63 mutant had a strongly reduced binding to DNA and in presence of the wild-type p63 protein the binding was not restored (Fig. 10A).
So we extended this analysis to others AEC mutants G534V, C519R, D544Y, E570fsX94 and N620fsX44. Similar ChIP analysis revealed that all mutants had an impaired ability to bind DNA, while the SHFM Q630X and E635X did not, suggesting that this is the reason why AEC mutants have an impaired transactivation ability.
To understand if SAM or PS domains are involved in the DNA binding, we performed ChIP with p63ΔSAM and p63ΔPS. Unexpectedly, but in accordance with the results of transactivation activity, p63ΔSAM had an impaired DNA binding, while p63ΔPS did not (Fig. 10B).
To verify the correlation between the transactivation assays performed with Krt14 promoter and the results of impaired binding to DNA, we also tested the ability of the mutants to bind to Krt14 enhancer (98). Similarly to the other tested enhancer, AEC mutants and p63ΔSAM, but not the SHFM mutants and p63ΔPS, had a reduced DNA binding (Fig. 10C).

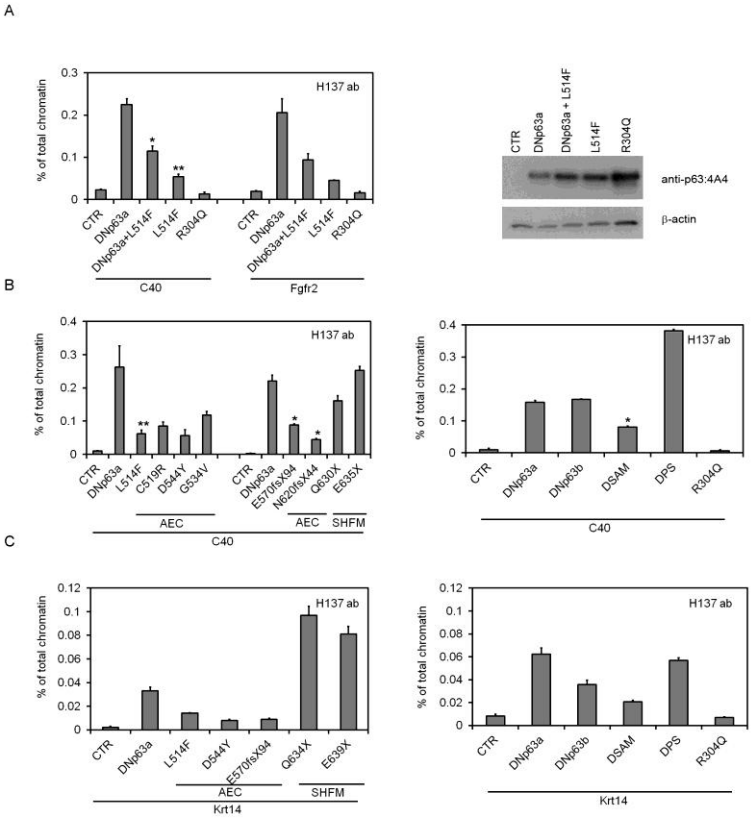

Figure 10: AEC p63 mutants and ΔSAM have a reduced DNA binding ability. (A) ChIP assay of wild-type and L514F ΔNp63α transfected in HEK293FT alone or in combination on C40 and Fgfr2 p63 binding sites reveals that L514F p63 mutant has an impairment in DNA binding ability, also in combination with wild-type protein. EEC mutant R304Q is used as negative control of DNA binding. The picture is representative of at least four independent experiments. On the right side of picture western blot analysis of p63 mutants revealed with anti-p63 4A4 antobodies and normalized for β-actin. *=0.01, **=0.0007. (B) On the left side, ChIP assay of AEC and SHFM p63 mutants transfected in HEK293FT cells on C40 binding site reveals that AEC p63 mutants have a reduced binding to DNA, while SHFM p63 mutants do not. The picture is representative of at least three independent experiments. *<0.01. On the right side, ChIP assay

performed on C40 binding site reveals that p63ΔSAM, but not p63ΔPS, has a reduced DNA binding ability. The picture is representative of at least four independent experiments. *=0.005. (C) ChIP assays of AEC, SHFM (on left side) and deleted p63 mutants (on right side) are performed on Krt14 p63 binding site and reveled that AEC p63 mutants and p63ΔSAM have an impairment in binding also this region. ab= antibodies; AEC= ankyloblepharon-ectodermal defects-cleft lip/palate syndrome; SHFM= split hand/foot malformation; DSAM= p63ΔSAM; ΔPS= p63ΔPS; CTR= negative control.

To confirm these results, in collaboration with Prof. Satrajit Sinha (Department of Biochemistry, Center of Excellence in Bioinformatics & Life Science, SUNY at Buffalo, NY), we performed an EMSA analysis on nuclear extract of HEK293 cells transfected with AEC mutants and p63ΔSAM and p63ΔPS. Binding was tested on an oligonucleotide corresponding to Krt14 enhancer and was observed with the wild-type protein but not the R304Q DNA binding mutant used as negative control. Interestingly, L514F, E570fsX94, N620fsX44 and p63ΔSAM had a reduced binding and to a lesser extent G534V, while not p63ΔPS. To demonstrate the binding specificity, we verified the supershift with an anti-p63 antibodies that recognizes the ΔN-specific region (RR-14) (Fig. 11).
These results indicate that AEC mutants bind DNA less efficiently than wild-type protein. Reduced binding was confirmed on various p63 DNA binding region with different assays. SAM domain seems to be required for binding, while PS domain do not, indeed only the lack of the first impaired this ability.

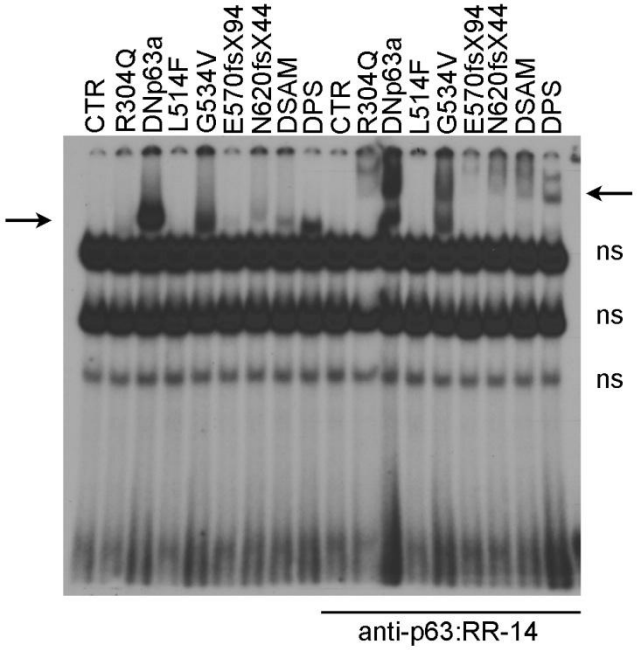

Figure 11: AEC p63 mutants and p63DSAM fail to bind an oligonucleotide corresponding to Krt14 enhancer. EMSA assay of nuclear extract of HEK293 cells transfected with ΔNp63α, AEC p63 mutants, p63ΔSAM and p63ΔPS reveals that L514F, E570fsX94, N620fsX44 and p63ΔSAM have a reduced binding and to a lesser extend G534V, while not p63ΔPS. In the second half of gel same extracts are incubated with an anti-p63 antibodies that recognizes the ΔN-specific region (RR-14) and the specificity of binding is demonstrated by supershift. Black arrows indicate shift (left) and supershift (right). ns: non specific.

3.4 Impaired gene expression of several target genes in AEC mutant heterozygous and homozygous keratinocytes

Since HEK293 cells do not express p63, to test the physiological significance of our findings we analyzed the effect of an endogenous L514F p63 mutant in primary keratinocytes.

To this aim we took advantage of a conditional knock-in mouse model ($p63^{+/floxL514F}$) recently generated in our laboratory, in which the L514F mutation is expressed only in the presence of the Cre recombinase. A 3xFLAG tag was cloned at the C-terminus of the mutant gene. The construct was inserted by recombination in murine embryonic stem (ES) cells (Fig.12A).
Primary keratinocytes obtained from homozygous and heterozygous mice for the mutation were infected with adenovirus carring a Cre-recombinase to activate the mutation. Adenovirus carring a GFP protein was used as control. At two (data not shown) and four days after infection we performed ChIP assays in primary keratinocytes with two different anti-p63 antibody, H137, that recognizes all p63 isoforms and H129, that recognizes only the alpha-isoform involved in AEC syndrome. AEC mutant was significantly impaired in DNA binding by itself and, to a lesser extent, in the presence of the wild-type protein, in accordance with the data obtained in heterologous system (Fig. 12B).
To assess the effects of this reduced DNA binding, RNAs from keratinocytes were collected two and four days after infection to evaluate changes in gene expression both soon after expression of mutated proteins and after few days. Different known p63 target genes were measured, such as Fgfr2 (88), Krt14 and Krt5 (99), Irf6 (100), Dsc3 and Dsp (89). In homozygous keratinocytes $p63^{L514F/L514F}$ we observed a strongly decreased expression of all the analyzed genes both after two and after four days. In heterozygous keratinocytes $p63^{+/L514F}$ the most affected genes was IRF6 and Fgfr2, in which a strongly reduction in their expression was evident after two and four days of infection (Fig. 12C).
These results indicate that even in its natural context AEC mutant has a reduced DNA binding not only in homozygous keratinocytes but also in heterozygous ones and that the consequence of this impairment is the reduced expression of different p63 target genes.

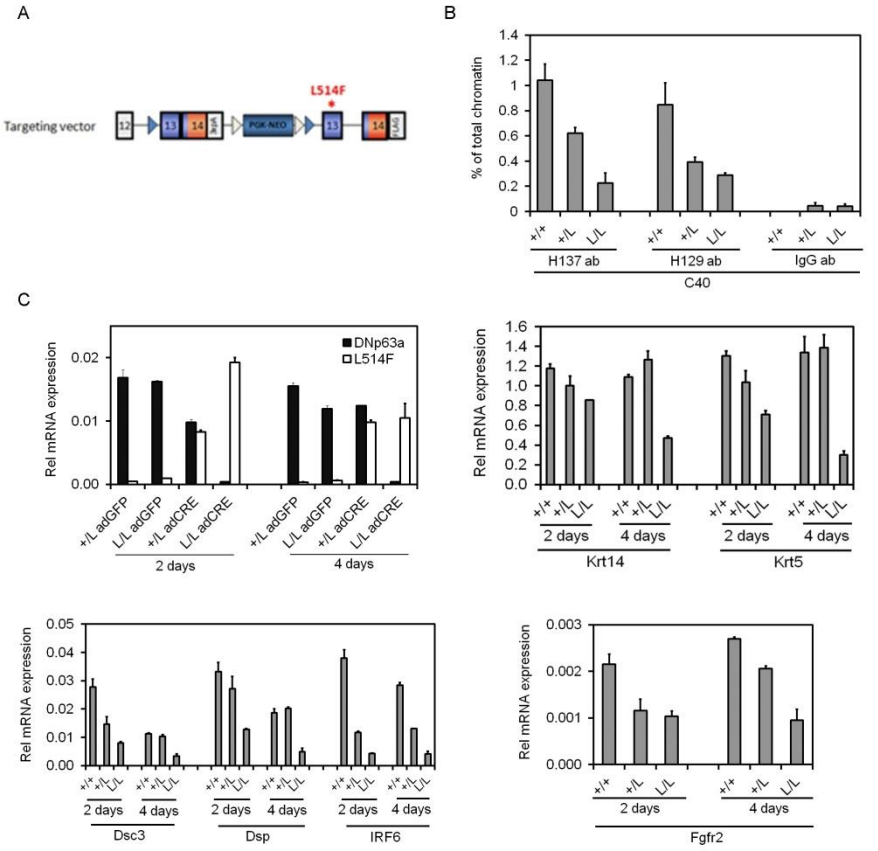

Figure 12: Reduced expression levels of several target genes in AEC mutant keratinocytes. (A) Gene targeting strategy used to generate the $p63^{+/floxL514F}$ inducible knock-in mice. The L514F mutation is indicated with *. Blue and white triangles indicate Lox and Flip sites respectively. A 3xFLAG tag was cloned at the C-terminus of the mutant gene. (B) ChIP assay performed on C40 four days after infection with two different anti-p63 antibodies, H137, that recognizes all p63 isoforms and H129, that recognizes only the alpha-isoform, reveals that both in heterozygous and mainly in homozygous keratinocytes DNA binding is reduced. IgG ab is used as negative control. ab= antibodies; L= L514F. (C) After controlling the right expression of p63 wild-type and L514F in keratinocytes treated with adenoGFP and adenoCRE (left side), RT real-time PCR of collected RNA from heterozygous and homozygous keratinocytes reveals

impaired gene expression of Krt14, Krt5, Dsc3, Dsp, IRF6 and Fgfr2 at two and four days after infection.

3.5 $p63^{-/L514F}$ mice have a perinatal lethal phenotype closely resembling the p63 null ones

Mice heterozygous for p63 ($p63^{+/-}$) are indistinguishable from wild-type littermates because one copy of all p63 isoforms is sufficient to maintain the ectodermal development in mice.
To better understand the mechanism of action of L514F p63 protein, we mated $p63^{+/-}$ mice with the knock-in $p63^{+/L514F}$ ones to obtain $p63^{-/L514F}$ mice. ChIP assay in E14.5 embryo skin of $p63^{+/L514F}$, $p63^{-/L514F}$ and wild-type using anti-p63 antibody (H137) revealed that L514F mutant p63 had an impairment in binding DNA on p63 enhancer element (Fig. 13A).
Sagittal views of E18.5 $p63^{-/L514F}$ mice showed an evident phenotype with cleft palate, craniofacial abnormalities and forelimbs and hindlimbs defects. $p63^{-/L514F}$ and $p63^{-/-}$ embryos had no eyelids, whisker pads, skin and related appendages, which are present on the wild-type control. $p63^{-/-}$ embryos lacks both forelimbs and hindlimbs as already reported by Mills et al., 1999 and Yang et al., 1999 (9, 10). In the $p63^{-/L514F}$ embryos hindlimbs were absent similarly to the knock-out, whereas forelimbs were more developed but still abnormal (Fig. 13B).
To analyze the effects of the AEC mutation on the skin phenotype, we performed an hematoxilin and eosin staining on skin sections. While $p63^{+/L514F}$ epidermis was hypoplastic as already described by Ferone et al., 2011 (68), in $p63^{-/L514F}$ the epidermal layers were disorganized, discontinuous and often detached from the dermis, similarly to the $p63^{-/-}$ (Fig. 13C).
These findings indicate that at least an intact α isoform is essential for epidermal, limbs and craniofacial development and that L514F mutation affects all these functions due to an impairment in DNA binding on p63 target genes.

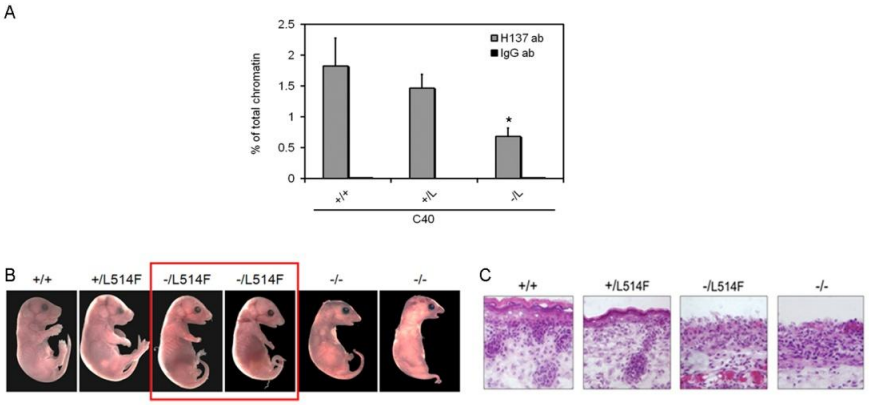

Figure 13: $p63^{-/L514F}$ mice closely resembling the p63 null ones. (A) ChIP assay performed on C40 p63 binding site of E14.5 skin embryos with anti-p63 antibodies, H137, reveals that in knock-out/L514F embryos DNA binding is reduced. ab= antibodies; L= L514F. *=0.0013. (B) Sagittal views of E18.5 $p63^{+/+}$, $p63^{+/L514F}$, $p63^{-/L514F}$, $p63^{-/-}$ mice showed for $p63^{-/L514F}$ (red square) an evident phenotype with cleft palate, craniofacial abnormalities and forelimbs and hindlimbs defects. (C) H&E staining on skin sections of $p63^{+/+}$, $p63^{+/L514F}$, $p63^{-/L514F}$, $p63^{-/-}$ mice showed $p63^{+/L514F}$ hypoplastic epidermis while in $p63^{-/L514F}$ the epidermal layers were disorganized, discontinuous and often detached from the dermis, similarly to the $p63^{-/-}$.

3. DISCUSSION

p63 gene is a transcription factor, member of p53 gene family, crucial for the development and maintenance of squamous epithelia. It is specifically expressed in the basal layers of stratified epithelial tissues in which it is mainly involved in maintaining cell proliferation and cell adhesion (13, 11, 32, 33). Its expression decrease upon keratinocyte differentiation, suggesting that p63, through the balance of its isoforms, is required for initiating epithelial stratification (11, 28, 33) and concurrently it inhibits differentiation (19, 28).

ΔNp63α is the most abundant isoform in the skin (16) and one of the first genes to be specifically expressed in the surface ectoderm at E7.5-E8. It continues to be expressed during skin development and in the basal proliferative layer in postnatal life (11, 25, 16).

This isoform contains two additional domains not present in p53 and likely responsible for ΔNp63α functions p53-unlike (23, 36): a SAM domain and a PS domain, whose functions in the context of p63 remain still unknown. Very few interactors of p63 that bind the protein interaction module SAM are known, such as ABBP1 and Scaf4/rA4 (56) or Cables1 (57). About PS domain, it shows no homology to any known sequence and it seems to be involved in inhibition of transactivation ability by binding and masking the TA domain of p63 (58). Its function in ΔNp63α, in which lacks TA domain, remains completely unknown.

The study of these domains is of great interest as they are involved in an autosomal dominant disorder known as AEC syndrome.

AEC syndrome belongs to the ectodermal dysplasia pathology and it is characterize by ectodermal dysplasia, ankyloblepharon and cleft lip and/or cleft palate. It is caused by mutations that fall in the SAM or PS domains, in the first case they are mainly missense mutations, while in the PS domain frameshift mutations that elongate p63 protein predominate.

In this work we investigate the functional role of these two domains and their involvement in AEC pathogenesis, starting from the study of different mutations causative of this syndrome and analyzing the consequence of lack of SAM or PS domains in ΔNp63α's functions.

We found that missense mutations of SAM domain and frameshift mutations of PS domain impair transcriptional activation of Krt14, a

direct target gene of p63 physiologically expressed in basal keratinocytes (98), in luciferase assays performed in heterologous system. Moreover we observed a different behavior for p63 that lacks SAM or PS domain, this demonstrate that functions are not redundant for these two domains, indeed p63ΔSAM have a reduced capability to transactivate transcription, while p63ΔPS have a stronger activity than the wild-type ΔNp63α protein.

A possible explanation for the different behavior of SAM and PS domains is that the first is necessary for transactivation activity of ΔNp63α protein, indeed point mutations in this domain are sufficient to strongly reduced this ability. PS domain does not seem to be implicated in transactivation, indeed only large rearrangements, such as frameshift mutations that extend p63 protein, but not the deletion of the whole domain, are responsible for the reduction of activity. The different response to the transactivation assays of frameshift mutations and total deletion of PS domain suggest that elongation of p63 protein could disturb the role of near domains.

First we ensured that L514F p63 mutant retains the ability to tetramerize, condition required for DNA binding, and that ΔNp63αΔSAM and ΔNp63αΔPS are able to bind wild-type ΔNp63α protein, indicating that these two C-terminal domains are not involved in homodimerization of p63. Then we investigated the ability of AEC mutants and p63ΔSAM and p63ΔPS to bind DNA with ChIP assays in HEK293FT cells. This capacity was tested on different p63 binding sites, such as C40, Fgfr2 and Krt14, and indicate that AEC mutants bind DNA less efficiently than wild-type protein. Moreover the co-expression of wild-type and L514F mutant does not restore the binding to DNA, suggesting that AEC mutant sequesters the wild-type protein in a still possible tetramers not working, acting as a dominant negative. Similar experiments of ChIP were performed for the two deletion mutants and demonstrated that SAM domain seems to be required for binding, while the PS one does not, indeed only the lack of the first impaired DNA binding, in accordance with results of transactivation assays.

To test the physiological significance of our findings we analyzed the effect of an endogenous L514F p63 mutant in primary keratinocytes, evaluating DNA binding and measuring expression levels of p63 target genes. The results indicated that even in its natural context AEC

mutant has reduced DNA binding in both homozygous and heterozygous keratinocytes and that the consequence of this impairment is the decresead expression levels of different p63 target genes, such as IRF6, Fgfr2, Dsc3, Dsp, Krt5 and Krt14. The reduced binding to DNA also in heterozigous keratinocytes confirms that L514F p63 mutant protein acts as a dominant negative. This reduction in DNA binding could be explained with an intrinsic incompetence of the mutated protein to bind DNA or to recruit some co-factors necessary for the binding.

In the context of primary keratinocytes, the presence of two copies of all other p63 isoforms doesn't restore the transactivation ability of p63 impaired by AEC mutant protein, suggesting that wild-type α isoform is required for these functions. This observation was even clearer when we analyzed the effect of L514F p63 mutation in p63 heterozygous mice with one copy of p63 isoforms. While $p63^{+/-}$ mice were indistinguishable from wild-type littermates because one copy of all p63 isoforms is sufficient to sustain the ectodermal development, $p63^{-/L514F}$ mice showed an evident phenotype with cleft palate, craniofacial abnormalities and forelimbs and hindlimbs defects, underlying the necessity of at least one copy of wild-type α isoforms.

Moreover in spite of an hypoplastic epidermis observed in $p63^{+/L514F}$ mice (68), in $p63^{-/L514F}$ the epidermal layers were disorganized, discontinuous and often detached from the dermis, similarly to the $p63^{-/-}$. At molecular level ChIP assays in E14.5 embryos $p63^{-/L514F}$ skin confirmed a L514F p63 mutant impairment in DNA binding. These findings indicate that at least one dose of intact α isoforms is essential for epidermal, limbs and craniofacial development, that β and γ isoforms can not rescue epidermal phenotype and that L514F mutation strongly affects all these phenotypes.

In this work we shed light on the mechanisms underlying AEC syndrome showing for the first time that all analyzed AEC mutants have an impairment in DNA binding causing a consequent reduction in the expression levels of different p63 target genes.

Moreover we demonstrate the different involvement in transactivation and DNA binding ability of two C-terminal domains of p63α isoform. In particular SAM domain seems to be required for these p63 functions, indeed its deletion, in spite of an intact DNA binding domain, results in a strong reduction in activating transcription of

Krt14 in luciferase assays and in an impaired DNA binding ability on all sites tested. This is not true for PS domain, in which the analyzed AEC causative frameshift mutations are responsible for described impairment but the deletion of whole domain does not, indicating that this domain is not involved in these functions.

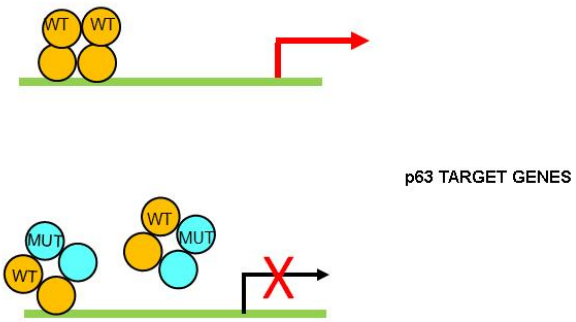

Fig. 14: Proposed model of mechanisms underlying AEC syndrome. AEC mutants have an impaired ability to bind DNA. The result of reduced binding is severe phenotype in mice as well as in humans due to decreased levels of p63 target genes.

REFERENCES

1. Koster MI, Kim S, Roop DR. p63 deficiency: a failure of lineage commitment or stem cell maintenance? J Investig Dermatol Symp Proc 2005 Nov; 10 (2): 118-23.
2. Chuong CM, Patel N, Lin J, Jung HS, Widelitz RB. Sonic hedgehog signaling pathway in vertebrate epithelial appendage morphogenesis: perspectives in development and evolution. Cell Mol Life Sci 2000 57: 1672-1681.
3. Rook A, Burns T. Rook's textbook of dermatology (Blackwell Science, Malden, Mass.) 2004 7th Ed p 4 v. (paged continuously).
4. Watt, FM. The stem cell compartment in human interfollicular epidermis. J Dermatol Sci 2002 28: 173–180.
5. Cotsarelis, G, Sun, TT, Lavker, RM. Label-retaining cells reside in the bulge area of pilosebaceous unit: Implications for follicular stem cells, hair cycle, and skin carcinogenesis. Cell 1990 61: 1329–1337.
6. Bickenbach, JR, Grinnell, KL. Epidermal stem cells: Interactions in developmental environments. Differentiation 2004 72: 371–380.
7. Rice, RH, Green, H. The cornified envelope of terminally differentiated human epidermal keratinocytes consists of cross-linked protein. Cell 1977 11: 417–422.
8. Dhouailly, D, Prin, F, Kanzler, B, Viallet, JP: Variations of cutaneous appendages: Regional specification and cross-species signals. In: Chuong CM (ed). Molecular Basis of Epithelial Appendage Morphogenesis 1998 Austin, TX: R. G. Landes, p 45–56.
9. Mills, AA, Zheng, B, Wang, XJ, Vogel, H, Roop, DR, Bradley, A. p63 is a p53 homologue required for limb and epidermal morphogenesis. Nature 1999 398: 708–713.
10. Yang A, Schweitzer R, Sun D, Kaghad M, Walker N, Bronson RT, Tabin C, Sharpe A, Caput D, Crum C, McKeon F. p63 is essential for regenerative proliferation in limb, craniofacial and epithelial development. Nature 1999 398: 714–718.
11. Koster, MI, Kim, S, Mills, AA, DeMayo, FJ, Roop, DR. p63 is the molecular switch for initiation of an epithelial stratification program. Genes Dev 2004 18: 126–131.
12. Yang, A, Kaghad, M, Caput, D, McKeon, F. On the shoulders of giants: p63, p73 and the rise of p53. Trends Genet 2002 18: 90–95.
13. Yang A, Zhu Z, Kapranov P, McKeon F, Church GM, Gingeras TR, Struhl K. Relationships between p63 binding, DNA sequence, transcription activity, and biological function in human cells. Mol Cell 2006 24: 593-602.
14. Kemp CJ, Wheldon T, & Balmain A. p53-deficient mice are extremely susceptible to radiation-induced tumorigenesis. Nat Genet 1994 8(1): 66-69.
15. Yang A, Walker N, Bronson R, Kaghad M, Oosterwegel M, Bonnin J, Vagner C, Bonnet H, Dikkes P, Sharpe A, McKeon F, Caput D. p73-

deficient mice have neurological, pheromonal and inflammatory defects but lack spontaneous tumours. Nature 2000 404(6773): 99-103.

16. Yang A, Kaghad M, Wang Y, Gillett E, Fleming MD, Dötsch V, Andrews NC, Caput D, McKeon F. p63, a p53 homolog at 3q27-29, encodes multiple products with transactivating, death-inducing, and dominant-negative activities. Mol Cell 1998 2(3): 305-316.
17. Helton ES, Zhu J, Chen X. The unique NH2-terminally deleted (DeltaN) residues, the PXXP motif, and the PPXY motif are required for the transcriptional activity of the DeltaN variant of p63. J Biol Chem 2006 281: 2533-2542.
18. Dohn, M, Zhang, S, Chen, X. p63alpha and DeltaNp63alpha can induce cell cycle arrest and apoptosis and differentially regulate p53 target genes. Oncogene 2001 **20**: 3193–3205.
19. King, KE, Ponnamperuma, RM, Yamashita, T, Tokino, T, Lee, LA, Young, MF, Weinberg, WC. deltaNp63alpha functions as both a positive and a negative transcriptional regulator and blocks in vitro differentiation of murine keratinocytes. Oncogene 2003 22: 3635–3644.
20. Wu G, Nomoto S, Hoque MO, Dracheva T, Osada M, Lee CC, Dong SM, Guo Z, Benoit N, Cohen Y, Rechthand P, Califano J, Moon CS, Ratovitski E, Jen J,Sidransky D, Trink B. DeltaNp63alpha and TAp63alpha regulate transcription of genes with distinct biological functions in cancer and development. Cancer Res 2003 63: 2351–2357.
21. Ghioni, P, Bolognese, F, Duijf, PH, van Bokhoven, H, Mantovani, R, Guerrini, L. Complex transcriptional effects of p63 isoforms: Identification of novel activation and repression domains. Mol Cell Biol 2002 22: 8659–8668.
22. Chi, SW, Ayed, A, Arrowsmith, CH. Solution structure of a conserved C-terminal domain of p73 with structural homology to the SAM domain. EMBO J 1999 18: 4438–4445.
23. Thanos, CD, Bowie, JU. p53 Family members p63 and p73 are SAM domain-containing proteins. Protein Sci 1999 8: 1708–1710.
24. Serber Z, Lai HC, Yang A, Ou HD, Sigal MS, Kelly AE, Darimont BD, Duijf PH, Van Bokhoven H, McKeon F, Dötsch V. A C-terminal inhibitory domain controls the activity of p63 by an intramolecular mechanism. Mol Cell Biol 2002 22: 8601–8611.
25. Laurikkala J, Mikkola ML, James M, Tummers M, Mills AA, Thesleff I. p63 regulates multiple signalling pathways required for ectodermal organogenesis and differentiation. Development 2006 133: 1553-1563.
26. Bamberger C, Schmale H. Identification and tissue distribution of novel KET/p63 splice variants. FEBS Lett. 2001 Jul 20;501(2-3): 121-6.
27. Liefer KM, Koster MI, Wang XJ, Yang A, McKeon F, Roop DR Down-regulation of p63 is required for epidermal UV-B-induced apoptosis. Cancer Res 2000 60: 4016-4020.
28. Nguyen BC[1], Lefort K, Mandinova A, Antonini D, Devgan V, Della Gatta G, Koster MI, Zhang Z, Wang J, Tommasi di Vignano A, Kitajewski J, Chiorino G, Roop DR, Missero C, Dotto GP. Cross-regulation between

Notch and p63 in keratinocyte commitment to differentiation. Genes Dev 2006 20: 1028-1042.

29. Parsa R, Yang A, McKeon F, Green H. Association of p63 with proliferative potential in normal and neoplastic human keratinocytes. J Invest Dermatol 1999 113: 1099-1105.
30. Pellegrini G, Dellambra E, Golisano O, Martinelli E, Fantozzi I, Bondanza S, Ponzin D, McKeon F, De Luca M. p63 identifies keratinocyte stem cells. Proc Natl Acad Sci U S A 2001 98: 3156-3161.
31. Westfall, MD, Mays, DJ, Sniezek, JC, Pietenpol, JA. The Delta Np63 alpha phosphoprotein binds the p21 and 14-3-3 sigma promoters *in vivo* and has transcriptional repressor activity that is reduced by Hay–Wells syndrome-derived mutations. Mol Cell Biol 2003 23: 2264–2276.
32. Sbisa E, Mastropasqua G, Lefkimmiatis K, Caratozzolo MF, D'Erchia AM, Tullo A. Connecting p63 to cellular proliferation: the example of the adenosine deaminase target gene. Cell Cycle 2006 5: 205-212.
33. Truong AB, Kretz M, Ridky TW, Kimmel R, Khavari PA. p63 regulates proliferation and differentiation of developmentally mature keratinocytes. Genes Dev 2006 20:185-3197.
34. Kaghad M, Bonnet H, Yang A, Creancier L, Biscan JC, Valent A, Minty A, Chalon P, Lelias JM, Dumont X, Ferrara P, McKeon F, Caput D. Monoallelically expressed gene related to p53 at 1p36, a region frequently deleted in neuroblastoma and other cancer. Cell 1997 90: 809–819.
35. De Laurenzi V, Costanzo A, Barcaroli D, Terrinoni A, Falco M, Annicchiarico-Petruzzelli M, Levrero M, Melino G. Two new p73 splice variants, gamma and delta, with different transcriptional activity. J. Exp. Med. 1998 188: 1763–1768.
36. Bork, P. and Koonin, E. V. Predicting functions from protein sequences-where are the bottlenecks? Nat. Genet. 1998 18: 313–318.
37. Ou HD, Löhr F, Vogel V, Mäntele W, Dötsch V. Structural evolution of C-terminal domains in the p53 family. EMBO J. 2007 Jul 25; 26(14): 3463-73.
38. Schultz, J., Ponting, C. P., Hofmann, K., and Bork, P. SAM as a protein interaction domain involved in development regulation. Protein Sci 1997 6: 249–253.
39. Hirai H, Maru Y, Hagiwara K, Nishida J, Takaku F. A novel putative tyrosine kinase receptor encoded by the eph gene. Science. 1987 Dec 18;238(4834): 1717-20.
40. Tessier-Lavigne M. Eph receptor tyrosine kinases, axon repulsion, and the development of topographic maps. Cell. 1995 Aug 11; 82(3): 345-8.
41. Kyba M, Brock HW. The SAM domain of polyhomeotic, RAE28, and scm mediates specific interactions through conserved residues. Dev Genet. 1998; 22(1): 74-84.
42. Sakane F, Kai M, Wada I, Imai S, Kanoh H. The C-terminal part of diacylglycerol kinase alpha lacking zinc fingers serves as a catalytic domain. Biochem J. 1996 Sep 1;318 (Pt 2): 583-90.
43. Ponting CP. SAM: a novel motif in yeast sterile and Drosophila polyhomeotic proteins. Protein Sci. 1995 Sep;4(9):1928-30.

44. Therrien M, Wong AM, Rubin GM. CNK, a RAF-binding multidomain protein required for RAS signaling. Cell. 1998 Oct 30;95(3): 343-53.
45. Qiao F, Bowie JU. The many faces of SAM. Sci STKE 2005 (286):re7.
46. McGrath JA, Duijf PH, Doetsch V, Irvine AD, de Waal R, Vanmolkot KR, Wessagowit V, Kelly A, Atherton DJ, Griffiths WA, Orlow SJ, van Haeringen A, Ausems MG, Yang A, McKeon F, Bamshad MA, Brunner HG, Hamel BC, van Bokhoven H. Hay-Wells syndrome is caused by heterozygous missense mutations in the SAM domain of p63. Hum Mol Genet 2001 10: 221–229.
47. Kantaputra PN, Hamada T, Kumchai T, McGrath JA. Heterozygous mutation in the SAM domain of p63 underlies Rapp-Hodgkin ectodermal dysplasia. J Dent Res 2003 82: 433–437.
48. Kim CA, Phillips ML, Kim W, Gingery M, Tran HH, Robinson MA, Faham S, Bowie JU. Polymerization of the SAM domain of TEL in leukemogenesis and transcriptional repression. Embo J 2001 20: 4173–4182.
49. Boccuni P, MacGrogan D, Scandura JM, Nimer SD. The human L(3)MBT polycomb group protein is a transcriptional repressor and interacts physically and functionally with TEL (ETV6). J Biol Chem 2003 278: 15412–15420.
50. Tognon CE, Mackereth CD, Somasiri AM, McIntosh LP, Sorensen PH. Mutations in the SAM domain of the ETV6-NTRK3 chimeric tyrosine kinase block polymerization and transformation activity. Mol Cell Biol 2004 24: 4636–4650.
51. Stapleton, D., Balan, I., Pawson, Y., and Sicheri, F. The crystal structure of an Eph receptor SAM domain reveals a mechanism for modular dimerization. Nat. Struct. Biol. 1999 6: 44–49.
52. Thanos, C. D., Goodwill, K. E., and Bowie, J. U. Oligomeric structure of the human EphB2 receptor SAM domain. Science 1999 283: 833–836.
53. Serra-Pages, C., Kedersha, N. L., Fazikas, L., Medley, Q., Debant, A., and Streuli, M. The LAR transmembrane protein tyrosine phosphatase and a coiled-coil LAR interacting protein co-localize at focal adhesions. EMBO J. 1995 14: 2827–2838.
54. Cicero DO, Falconi M, Candi E, Mele S, Cadot B, Di Venere A, Rufini S, Melino G, Desideri A. NMR structure of the p63 SAM domain and dynamical properties of G534V and T537P pathological mutants, identified in the AEC syndrome. Cell Biochem Biophys 2006 44(3): 475-489.
55. Sathyamurthy A, Freund SM, Johnson CM, Allen MD, Bycroft M. Structural basis of p63α SAM domain mutants involved in AEC syndrome. FEBS J. 2011 278(15): 2680-8. doi: 10.1111/j.1742.
56. Fomenkov A, Huang YP, Topaloglu O, Brechman A, Osada M, Fomenkova T, Yuriditsky E, Trink B, Sidransky D, Ratovitski E. P63 alpha mutations lead to aberrant splicing of keratinocyte growth factor receptor in the Hay-Wells syndrome. J Biol Chem. 2003 Jun 27 278(26): 23906-14.
57. Wang XJ, Cao Q, Liu X, Wang KT, Mi W, Zhang Y, Li LF, LeBlanc AC, Su XD. Crystal structures of human caspase 6 reveal a new mechanism for intramolecular cleavage self-activation. EMBO Rep. 2010 Nov 11(11): 841-7.

58. Straub WE, Weber TA, Schäfer B, Candi E, Durst F, Ou HD, Rajalingam K, Melino G, Dötsch V. The C-terminus of p63 contains multiple regulatory elements with different functions. Cell Death Dis. 2010 1:e5.
59. Levine, A. J. p53, the cellular gatekeeper for growth and division. Cell 1997 88: 323–331.
60. Davison, T. S., C. Vagner, M. Kaghad, A. Ayed, D. Caput, and C. H. Arrowsmith. p73 and p63 are homotetramers capable of weak heterotypic interactions with each other but not with p53. J. Biol. Chem. 1999 274: 18709– 18714.
61. Kim DA, Lee BL, Suh EK. Ionizing radiation-induced TAp63α phosphorylation at C-terminal S/TQ motifs requires the N-terminal transactivation (TA) domain. Cell Cycle. 2011 Mar 1 10(5): 840-9.
62. Sayan BS, Sayan AE, Yang AL, Aqeilan RI, Candi E, Cohen GM, Knight RA, Croce CM, Melino G. Cleavage of the transactivation-inhibitory domain of p63 by caspases enhances apoptosis. Proc Natl Acad Sci U S A. 2007 Jun 26;104(26):10871-6.
63. Ghioni P, D'Alessandra Y, Mansueto G, Jaffray E, Hay RT, La Mantia G, Guerrini L. The protein stability and transcriptional activity of p63alpha are regulated by SUMO-1 conjugation. Cell Cycle 2005; 4: 183–190.
64. Ross S, Best JL, Zon LI, Gill G. SUMO-1 modification represses Sp3 transcriptional activation and modulates its subnuclear localization. Mol Cell 2002 10: 831–842.
65. Gill G. Something about SUMO inhibits transcription. Curr Opin Genet Dev 2005 15: 536–541.
66. Melchior F, Schergaut M, Pichler A. SUMO: ligases, isopeptidases and nuclear pores. Trends Biochem Sci 2003 28: 612–618.
67. Muller S, Hoege C, Pyrowolakis G, Jentsch S. SUMO, ubiquitin's mysterious cousin. Nat Rev Mol Cell Biol 2001 2: 202–210.
68. Senoo M, Pinto F, Crum CP, McKeon F. p63 Is essential for the proliferative potential of stem cells in stratified epithelia. Cell 2007 129: 523-536.
69. Romano RA, Ortt K, Birkaya B, Smalley K, Sinha S. An active role of the DeltaN isoform of p63 in regulating basal keratin genes K5 and K14 and directing epidermal cell fate. PLoS One 2009 4: e5623.
70. Rinne T, Brunner HG, van Bokhoven H. p63-associated disorders. Cell Cycle. 2007 Feb 1 6(3): 262-8.
71. Rinne T, Hamel B, Bokhoven H, Brunner HG. Pattern of p63 mutations and their phenotypes-update. Am J Med Genet A 2006 140: 1396-1406.
72. Celli J, Duijf P, Hamel BC, Bamshad M, Kramer B, Smits AP, Newbury-Ecob R, Hennekam RC, Van BG, van HA, Woods CG, van Essen AJ, de WR, Vriend G, Haber DA, Yang A, McKeon F, Brunner HG, van BH. Heterozygous germline mutations in the p53 homolog p63 are the cause of EEC syndrome. Cell 1999 99: 143-153.
73. Bertola DR, Kim CA, Albano LM, Scheffer H, Meijer R, van BH. Molecular evidence that AEC syndrome and Rapp-Hodgkin syndrome are variable expression of a single genetic disorder. Clin Genet 2004 66:79-80.

74. van Bokhoven H and Brunner HG. Splitting p63. Am J Hum Genet 2002 71:1-13.68.
75. Barrow LL, van BH, ack-Hirsch S, Andersen T, van Beersum SE, Gorlin R, Murray JC. Analysis of the p63 gene in classical EEC syndrome, related syndromes, and non-syndromic orofacial clefts. J Med Genet 2002 39: 559-566.
76. Bougeard G, Hadj-Rabia S, Faivre L, Sarafan-Vasseur N, Frebourg T. The Rapp-Hodgkin syndrome results from mutations of the TP63 gene. Eur J Hum Genet 2003 11: 700-704.
77. Dianzani I, Garelli E, Gustavsson P, Carando A, Gustafsson B, Dahl N, Anneren G. Rapp- Hodgkin and AEC syndromes due to a new frameshift mutation in the TP63 gene. J Med Genet 2003 40: e133.
78. Tsutsui K, Asai Y, Fujimoto A, Yamamoto M, Kubo M, Hatta N. A novel p63 sterile alpha motif (SAM) domain mutation in a Japanese patient with ankyloblepharon, ectodermal defects and cleft lip and palate (AEC) syndrome without ankyloblepharon. Br J Dermatol 2003 149: 395-399.
79. Chan I, McGrath JA, Kivirikko S. Rapp-Hodgkin syndrome and the tail of p63. Clin Exp Dermatol 2005 30: 183-186.
80. Shotelersuk V, Janklat S, Siriwan P, Tongkobpetch S. De novo missense mutation, S541Y, in the p63 gene underlying Rapp-Hodgkin ectodermal dysplasia syndrome. Clin Exp Dermatol 2005 30: 282-285.
81. Kannu P, Savarirayan R, Ozoemena L, White SM, McGrath JA. Rapp-Hodgkin ectodermal dysplasia syndrome: the clinical and molecular overlap with Hay-Wells syndrome. Am J Med Genet A 2006 140: 887-891.
82. Sorasio L, Ferrero GB, Garelli E, Brunello G, Martano C, Carando A, Belligni E, Dianzani I, Cirillo SM. AEC syndrome: further evidence of a common genetic etiology with Rapp- Hodgkin syndrome. Eur J Med Genet. 2006 49(6): 520-2.
83. Duijf PH, Vanmolkot KR, Propping P, Friedl W, Krieger E, McKeon F, Dotsch V, Brunner HG, van Bokhoven H. Gain-of-function mutation in ADULT syndrome reveals the presence of a second transactivation domain in p63. Hum Mol Genet 2002 11: 799-804.
84. Leoyklang P, Siriwan P, Shotelersuk V. A mutation of the p63 gene in non-syndromic cleft lip. J Med Genet 2006 43: e28.
85. Hay RJ., Wells RS. The syndrome of ankyloblepharon, ectodermal defects and cleft lip and palate: an autosomal dominant condition. Br J Dermatol 1976 94(3): 277-289.
86. Rinne T, Clements SE, Lamme E, Duijf PH, Bolat E, Meijer R, Scheffer H, Rosser E, Tan TY, McGrath JA, Schalkwijk J, Brunner HG, Zhou H, van Bokhoven H. A novel translation re-initiation mechanism for the p63 gene revealed by amino-terminal truncating mutations in Rapp-Hodgkin/Hay-Wells-like syndromes. Hum Mol Genet 2008 17(13): 1968-1977.
87. Browne G, Cipollone R, Lena AM, Serra V, Zhou H, van Bokhoven H, Dötsch V, Merico D, Mantovani R, Terrinoni A, Knight RA, Candi E, Melino G. Differential altered stability and transcriptional activity of

ΔNp63 mutants in distinct ectodermal dysplasias. J Cell Sci. 2011 Jul 1 124(Pt 13): 2200-7.

88. Ferone G, Thomason HA, Antonini D, De Rosa L, Hu B, Gemei M, Zhou H, Ambrosio R, Rice DP, Acampora D, van Bokhoven H, Del Vecchio L, Koster MI, Tadini G, Spencer-Dene B, Dixon M, Dixon J, Missero C. Mutant p63 causes defective expansion of ectodermal progenitor cells and impaired FGF signalling in AEC syndrome. EMBO Mol Med. 2012 4(3): 192-205.
89. Ferone G, Mollo MR, Thomason HA, Antonini D, Zhou H, Ambrosio R, De Rosa L, Salvatore D, Getsios S, van Bokhoven H, Dixon J, Missero C. p63 control of desmosome gene expression and adhesion is compromised in AEC syndrome. Hum Mol Genet. 2013 22(3): 531-43.
90. De Moerlooze L, Williamson J, Liners F, Perret J, Parmentier M. Cloning and chromosomal mapping of the mouse and human genes encoding the orphan glucocorticoid-induced receptor (GPR83). Cytogenet Cell Genet. 2000 90(1-2): 146-50.
91. Petiot A, Conti FJ, Grose R, Revest JM, Hodivala-Dilke KM, Dickson C. A crucial role for Fgfr2-IIIb signalling in epidermal development and hair follicle patterning. Development. 2003 130(22): 5493-501.
92. Rice R, Spencer-Dene B, Connor EC, Gritli-Linde A, McMahon AP, Dickson C, Thesleff I, Rice DP. Disruption of Fgf10/Fgfr2b-coordinated epithelial–mesenchymal interactions causes cleft palate. J Clin Invest 2004 113: 1692-1700.
93. van Bokhoven H, Hamel BC, Bamshad M, Sangiorgi E, Gurrieri F, Duijf PH, Vanmolkot KR, van Beusekom E, van Beersum SE, Celli J, Merkx GF, Tenconi R,Fryns JP, Verloes A, Newbury-Ecob RA, Raas-Rotschild A, Majewski F, Beemer FA, Janecke A, Chitayat D, Crisponi G, Kayserili H, Yates JR, Neri G, Brunner HG. p63 Gene mutations in eec syndrome, limb-mammary syndrome, and isolated split hand-split foot malformation suggest a genotype-phenotype correlation. Am J Hum Genet. 2001 Sep 69(3): 481-92.
94. Candi E, Rufini A, Terrinoni A, Dinsdale D, Ranalli M, Paradisi A, De Laurenzi V, Spagnoli LG, Catani MV, Ramadan S, Knight RA, Melino G. Differential roles of p63 isoforms in epidermal development: selective genetic complementation in p63 null mice. Cell Death Differ. 2006 Jun 13(6): 1037-47.
95. Serra V, Castori M, Paradisi M, Bui L, Melino G, Terrinoni A. Functional characterization of a novel TP63 mutation in a family with overlapping features of Rapp-Hodgkin/AEC/ADULT syndromes. Am J Med Genet A. 2011 Dec 155A(12): 3104-9.
96. Deutsch GB, Zielonka EM, Coutandin D, Weber TA, Schäfer B, Hannewald J, Luh LM, Durst FG, Ibrahim M, Hoffmann J, Niesen FH, Sentürk A, Kunkel H,Brutschy B, Schleiff E, Knapp S, Acker-Palmer A, Grez M, McKeon F, Dötsch V. DNA damage in oocytes induces a switch of the quality control factor TAp63α from dimer to tetramer. Cell. 2011 144(4): 566-76.

97. Antonini D., Rossi B., Han R., Minichiello A., Di Palma T., Corrado M.,Banfi S., Zannini MS., Brissette JL., and Missero C. An Autoregulatory Loop Directs the Tissue-Specific Expression of *p63* through a Long-Range Evolutionarily Conserved Enhancer. Mol Cell Biol. 2006 April 26(8): 3308–3318.
98. Romano RA, Birkaya B, Sinha S. A Functional Enhancer of Keratin14 Is a Direct Transcriptional Target of DNp63. J Invest Dermatol. 2007 May 127(5): 1175-86.
99. Romano RA, Ortt K, Birkaya B, Smalley K, Sinha S. An Active Role of the DN Isoform of p63 in Regulating Basal Keratin Genes K5 and K14 and Directing Epidermal Cell Fate. PLoS One. 2009 May 20 4(5): e5623.
100. Moretti F, Marinari B, Lo Iacono N, Botti E, Giunta A, Spallone G, Garaffo G, Vernersson-Lindahl E, Merlo G, Mills AA, Ballarò C, Alemà S, Chimenti S, Guerrini L, Costanzo A. A regulatory feedback loop involving p63 and IRF6 links the pathogenesis of 2 genetically different human ectodermal dysplasias. J. Clin. Invest. 2010 120: 1570–1577.
101. Romano RA, Birkaya B, Sinha S. Defining the Regulatory Elements in the Proximal Promoter of ΔNp63 in Keratinocytes: Potential Roles for Sp1/Sp3, NF-Y, and p63. J Invest Dermatol. 2006 Jul;126(7):1469-79.
102. Cheng W, Jacobs WB, Zhang JJ, Moro A, Park JH, Kushida M, Qiu W, Mills AA, Kim PC. ΔNp63 plays an anti-apoptotic role in ventral bladder development. Development. 2006 Dec 133(23): 4783-92.

The Desmosomal Protein Desmoglein 1 Aids Recovery of Epidermal Differentiation after Acute Ultraviolet Light Exposure OPEN

Jodi L Johnson, Jennifer L Koetsier, Anna Sirico, Ada T Agidi, Dario Antonini, Caterina Missero, Kathleen J Green

Cite this article as: Jodi L Johnson, Jennifer L Koetsier, Anna Sirico, Ada T Agidi, Dario Antonini, Caterina Missero, Kathleen J Green, The Desmosomal Protein Desmoglein 1 Aids Recovery of Epidermal Differentiation after Acute Ultraviolet Light Exposure, *Journal of Investigative Dermatology* accepted article preview 4 March 2014; doi: 10.1038/jid.2014.124.

Received 8 January 2014; accepted 18 February 2014; Accepted article preview online 4 March 2014

The desmosomal protein Desmoglein 1 aids recovery of epidermal differentiation after acute ultraviolet light exposure

Jodi L. Johnson[1, 2], Jennifer L. Koetsier[1], Anna Sirico[4], Ada T. Agidi[3], Dario Antonini[4], Caterina Missero[4, 5], Kathleen J. Green[1, 2, §]

Department of Pathology[1] and Department of Dermatology[2], Northwestern University Feinberg School of Medicine, Chicago, IL 60611, USA; Department of Chemistry[3], Spelman College, Atlanta, GA 30314, USA; CEINGE Biotecnologie Avanzate, via G. Salvatore 486[4] and Department of Biology, University of Naples Federico II, via Cinthia 26[5] - 80145 Napoli, Italy

§ To whom correspondence should be addressed:

303 E Chicago Ave,

Chicago, IL 60611

Telephone: (312) 503-5300

Fax: (312) 503-8240

E-mail: kgreen@northwestern.edu

Recovery of differentiation after UV exposure

Abbreviations used: Dsc, desmocollin; Dsg, desmoglein; Ecad, E-cadherin; HDAC, histone deacetylase; K1/10, Keratin 1 or 10; Lor, loricrin; NHEK, normal human epidermal keratinocyte; Pg, plakoglobin; TSA, trichostatin A; UV, ultraviolet

Abstract:

Epidermal structure is damaged by exposure to ultraviolet (UV) light but the molecular mechanisms governing structural repair are largely unknown. UVB (290-320 nm wavelengths) exposure prior to induction of differentiation reduced expression of differentiation-associated proteins, including Desmoglein 1 (Dsg1), Desmocollin 1 (Dsc1) and Keratins 1 and 10 (K1/K10) in a dose-dependent manner in normal human epidermal keratinocytes (NHEKs). The UVB-induced reduction in both Dsg1 transcript and protein was associated with reduced binding of the p63 transcription factor to previously unreported enhancer regulatory regions of the Dsg1 gene. Since Dsg1 promotes epidermal differentiation in addition to participating in cell-cell adhesion, the role of Dsg1 in aiding differentiation after UVB damage was tested. Compared to controls, depleting Dsg1 via shRNA resulted in further reduction of Dsc1 and K1/K10 expression in monolayer NHEK cultures and in abnormal epidermal architecture in organotypic skin models recovering from UVB exposure. Ectopic expression of Dsg1 in keratinocyte monolayers rescued the UVB-induced differentiation defect. Treatment of UVB-exposed monolayer or organotypic cultures with Trichostatin A, a histone deacetylase inhibitor, partially restored differentiation marker expression, suggesting a potential therapeutic strategy for reversing UV-induced impairment of epidermal differentiation after acute sun exposure.

Introduction:

The epidermis is a multilayered structure that provides a barrier against environmental insults. However, all epidermal layers can be penetrated by ultraviolet (UV) light resulting in potentially mutagenic DNA damage (Courdavault *et al.*, 2005; Pfeifer and Besaratinia, 2012) and changes in epidermal structure. UV-induced histological changes include hyperplasia, appearance of "sunburn cells" (pyknotic nuclei, eosinophilic cytoplasm, lacking expression of differentiation markers), disappearance of the granular layer, parakeratosis (aberrant persistence of nuclei in the stratum corneum), and acanthosis (thickening) and hyperkeratinization of the stratum corneum, all indicative of abnormal differentiation and altered barrier function (Bayerl *et al.*, 1995; Bernerd and Asselineau, 1997; Lavker *et al.*, 1995; Lorincz, 1960; Matsumura and Ananthaswamy, 2004; Rosario *et al.*, 1979). The molecular pathways leading to repair of the epidermal structure and restoration of normal differentiation after UV exposure remain largely unknown.

Normal epidermal differentiation and barrier formation require the carefully choreographed expression of cytoskeletal, cell adhesion, and cell envelope proteins specific for each cell layer. UV exposure impairs the expression of later differentiation markers such as involucrin, loricrin, filaggrin, and transglutaminase, corresponding with the histologically observed reduction in the granular layer and disturbance of the stratum corneum (Bayerl *et al.*, 1995; Bernerd and Asselineau, 1997; Del Bino *et al.*, 2004; Gambichler *et al.*, 2008; Kwon *et al.*, 2008; Lee *et al.*, 2005; Lee *et al.*, 2002; Li *et al.*, 2001; Rundhaug *et al.*, 2005; Sesto *et al.*, 2002; van der Vleuten *et al.*, 1996). UV exposure also disrupts the epidermal permeability barrier and

cell-cell communication by altering the arrangement of the tight junction proteins occludin and claudins-1 and -4 (Robert *et al.*, 1999; Yuki *et al.*, 2011), the lipid composition in upper epidermal layers (Holleran *et al.*, 1997), and the localization of connexin 43 (Cx43) (Bellei *et al.*, 2008; Provost *et al.*, 2003).

Expression of both classic and desmosomal cadherins is also altered by UV exposure (Dusek *et al.*, 2006; Gambichler *et al.*, 2008; Hung *et al.*, 2006; Li *et al.*, 2001; Murakami *et al.*, 2001; Rundhaug *et al.*, 2005; Sesto *et al.*, 2002). Of particular interest is Desmoglein 1 (Dsg1), one of several desmosomal cadherins that complex with armadillo proteins (i.e. Plakoglobin – Pg and Plakophilins – Pkps), and plakins (e.g. Desmoplakin – Dp) to anchor keratin intermediate filaments to the cell membrane. Dsg1 is first expressed as keratinocytes transit from the basal to the immediate suprabasal layer and becomes increasingly concentrated in desmosomes of the granular layer where it plays a critical role in intercellular adhesion (Green and Simpson, 2007). The Dsg1 cytoplasmic domain also promotes epidermal differentiation and proper epidermal morphogenesis (Getsios *et al.*, 2009). Knocking down Dsg1 results in reduction of the granular layer in epidermal models and reduced expression of differentiation markers desmocollin 1 (Dsc1), loricrin, filaggrin, and keratin 10 (K10). Dsg1 mRNA transcripts have been reported as downregulated after UV exposure, one of many transcriptional changes that occur in UV-exposed keratinocytes (Murakami *et al.*, 2001; Rundhaug *et al.*, 2005). Further, exposure of well differentiated keratinocytes to UVC wavelengths (below 290 nm which do not reach the earth's surface) leads to cellular redistribution and caspase-dependent cleavage of Dsg1 protein (Dusek *et al.*, 2006). However, no study has yet examined the impacts of UVB wavelengths (290-320 nm that impact human skin) on the expression or function of Dsg1 protein in the epidermis.

Since Dsg1 promotes epidermal differentiation (Getsios *et al.*, 2009), we examined the role of Dsg1 in governing recovery of keratinocyte differentiation following UVB exposure. UVB exposure resulted in reduced expression of Dsg1, Dsc1, K10, and K1 expression in a dose-dependent manner but did not reduce the predominantly basally-expressed Dsg3 protein or the adherens junction cadherin E-cadherin (Ecad). UVB-induced reduction of Dsg1 mRNA and protein was associated with decreased binding of the transcription factor p63 to previously unreported enhancer regulatory regions of the Dsg1 gene. Dsg1 silencing resulted in further reduction in Dsc1, K1, and K10 protein expression and in abnormal epidermal architecture after UVB exposure while ectopic Dsg1 expression led to recovery of the differentiation program. These findings establish Dsg1 is a specific regulator of the epidermal recovery process after assault by UVB light. Dsg1 may therefore be a therapeutic target for restoration of epidermal differentiation after sun exposure. Indeed, the histone deacetylase (HDAC) inhibitor Trichostatin A (TSA), which was previously shown to increase expression of desmosomal cadherins (Simpson *et al.*, 2010a), partially rescued UVB-induced reduction in differentiation markers in both monolayer cells and organotypic epidermal models. HDAC inhibitors may therefore be useful treatments for enhancing epidermal differentiation after acute UVB exposure, with potential applications for skin cancer prevention.

Results:

Acute UVB exposure of keratinocytes prior to induction of differentiation results in decreased expression of differentiation-associated proteins: To examine the impact of UVB

exposure on differentiation-dependent desmosomal cadherins and keratins in early epidermal differentiation, normal human epidermal keratinocytes (NHEKs) were exposed to increasing dosages of UVB prior to switching to high calcium medium to induce differentiation. A reduction in both Dsg1 and Dsc1 was observed when NHEKs were exposed to 1000, 2000 or 3000 J/m^2 UVB prior to calcium switch, while other cadherins Dsg3 and Ecad were not affected (Fig. 1a). Differentiation-associated keratins K10 and K1 as well as Pg levels were also reduced after exposure to the higher UVB dosages. An increase in phosphorylated Erk (pErk) was observed at the same UVB dosages associated with decreased differentiation markers. Thus the viable cells remaining after acute UVB exposure exhibited an increase in pro-proliferative signaling (Dumesic *et al.*, 2009).

To determine the level of cell death induced by the acute UVB dosages, apoptotic cells were assessed using the Terminal deoxynucleotidyl transferase dUTP nick end labeling (TUNEL) assay 48 hours after UVB exposure. The remaining viable cells per microscopic field were also counted. 2000 J/m^2 UVB exposure resulted in less than 3% of cells undergoing apoptosis at the 48 hour time point and approximately 2/3 of the cells remaining compared to unexposed controls, while exposure to 3000 J/m^2 UVB resulted in approximately 8% of cells undergoing apoptosis and 1/3 of the cells remaining (Fig. 1b).

The morphology of organotypic cultures exposed to the same UVB regimen after differentiation and stratification had occurred was also analyzed for comparison (Supplemental Fig. 1 exposed on day 6 and harvested on day 7 after lifting, see timeline). Acanthosis of the stratum corneum and increased intercellular spaces, particularly in the lower epidermal layers,

were observed in the cultures exposed to 1000 J/m^2 UVB. Sunburn cells were apparent in the cultures exposed to 1500 J/m^2 and increased in number with the higher UVB dosages. The stratum corneum and granular layers, and the expression and distribution of Dsg1, Dsc1, and loricrin were disturbed in the cultures exposed to UVB dosages from 1500 to 3000 J/m^2, consistent with defects in differentiation.

Dsg1 promotes epidermal differentiation and architectural recovery after UVB exposure: We previously demonstrated that Dsg1 promotes epidermal differentiation through attenuation of Erk1/2 signaling (Getsios *et al.*, 2009). To address whether loss of Dsg1 exacerbates reduction in differentiation after UVB exposure, Dsg1 was depleted in NHEKs via shRNA. Knocking down Dsg1 resulted in more pronounced reductions in Dsc1, K10, and K1 at UVB dosages as low as 500 J/m^2 and almost total loss of detectable Dsc1, K10, or K1 proteins in NHEKS exposed to 2000 or 3000 J/m^2 UVB (Fig. 2a right). In control-infected NHEKs, as in uninfected NHEKs in Fig. 1, exposure to 2000 or 3000 J/m^2 UVB resulted in reduction of Dsg1, Dsc1, K10, and K1 (Fig. 2a left). Thus Dsg1 loss exacerbated the reduction in keratinocyte differentiation markers in a UVB dose-dependent manner.

To understand the impact of Dsg1 loss on the recovery of proper epidermal architecture after UVB exposure, organotypic cultures were grown from NHEKs infected with control or Dsg1 shRNA. The cultures were exposed to 1000 J/m^2 UVB on day 6 after lifting to the air-liquid interface and then allowed to recover for either 24 hours or 7 days (see timeline). In control-infected organotypic cultures, the number of cells staining positive for Dsg1 was reduced 24 hours after UVB exposure compared to unexposed cultures, but Dsg1 expression was restored

by the later time point (Fig 2b, left panels). Seven days after UVB exposure in the Dsg1-depleted organotypic cultures, the thickness of the viable epithelial portion was reduced compared to controls. A thickened, disorganized stratum corneum accumulated, exhibiting remnants of cell nuclei (Fig. 2b, right panels). Dsg1 was therefore important for recovery of proper epidermal model architecture after UVB exposure.

To determine whether increasing Dsg1 expression would help restore expression of other differentiation-associated proteins after UVB exposure, NHEKs were infected with viruses expressing either GFP control or ectopic Dsg1. Ectopic Dsg1 expression resulted in increased Dsc1, K10, and K1 expression 48 hours after UVB exposure compared to controls (Fig. 2c). The data indicated that Dsg1 was important for regulating expression of other differentiation markers after UVB exposure.

UVB-induced delay in differentiation and reduced Dsg1 mRNA levels are associated with decreased binding of p63 to regulatory regions upstream of the Dsg1 gene: The effects of UVB exposure on expression of differentiation markers could be at the level of protein stability, gene transcription, or both. To test whether UVB exposure resulted in a delay in induction of differentiation marker expression, NHEKs were either unexposed (Fig. 3a) or exposed to 2000 J/m^2 UVB (Fig. 3b) immediately prior to calcium switch to induce differentiation and harvested at 4 or 12 hour intervals beginning at 48 hours. While Dsg1 protein was detectable as early as 48 hours after calcium switch in the unexposed cells, it remained difficult to detect until 72 hours in the UVB-exposed NHEKs. Other differentiation markers Dsc1, K10, and K1 were detectable by 60 hours in the unexposed cells while remaining difficult to detect until 72 hours in the UVB-

exposed NHEKs. Quantitative RT-PCR revealed that Dsg1 transcript levels were reduced as early as 5 hours and remained reduced 72 hours after calcium switch in UVB-exposed NHEKs compared to unexposed controls.

The master regulator of epidermal differentiation, p63 (Koster, 2010), was recently shown to bind to a mouse Dsg1 gene regulatory region to induce Dsg1 transcription (Ferone *et al.*, 2013). Thus, we reasoned that p63-induced transcription of Dsg1 may be impacted by exposure of NHEKs to UVB. To identify p63 binding sites in the human Dsg1 genomic locus, previously generated ChIP-seq data obtained in human keratinocytes (Kouwenhoven *et al.*, 2010) were analyzed. Three p63-binding regions (-25Kb, -60Kb, -70Kb) were identified upstream of the gene and corresponded to genomic regions enriched in positive histone marks associated with active transcription, and to clusters of DNase hypersensitive sites (Supplemental Fig. 2a) (Bernstein *et al.*, 2005; Sabo *et al.*, 2006). Using Chromatin Immunoprecipitation (ChIP) to test binding of p63 to these putative regions resulted in the finding that p63 preferentially bound to the regulatory region 60kB from the human Dsg1 gene (Fig. 3d) and bound to a lesser extent to the other regions (Supplemental Fig. 2b). p63 binding to these regulatory regions was decreased following exposure of NHEKs to 2000 J/m^2 UVB (Fig. 3d and Supplemental Fig. 2b), correlating with the UVB-induced reduction in Dsg1 transcripts.

Treatment of cultures with the HDAC inhibitor TSA increases differentiation marker expression after UVB exposure: Since previous studies showed that treatment of cells with the HDAC inhibitor TSA increases expression of desmosomal cadherins (Simpson *et al.*, 2010a) experiments were conducted to determine if TSA treatment after UVB exposure would rescue

Dsg1 expression. Indeed, TSA treatment increased Dsg1 and Dsc1 expression in monolayer cultures (Supplemental Fig. 3) and Dsg1, Dsc1, and K10 expression in organotypic epidermal cultures (Fig. 4a) after UVB exposure compared to UVB-exposed untreated or DMSO treated controls. This was not through an increase in p63 binding to the Dsg1 gene regulatory regions (data not shown). TSA treatment also reduced UVB-induced phosphorylation of Erk compared to DMSO-treated controls (Fig 4b).

Discussion:

From these studies we conclude that Dsg1 promotes differentiation and structural repair of UVB-damaged epidermis. Further, our work shows that a clinically relevant HDAC inhibitor, TSA, increases Dsg1 expression and helps restore epidermal differentiation following acute UVB exposure. This work is important, as cumulative sun exposure and childhood sunburns significantly correspond with increased risk of skin carcinogenesis in adulthood (English *et al.*, 1998), and UV-induced alterations in epidermal structural proteins may contribute to retention of mutated cells within the skin structure that later become cancerous. For example, loss of Dsg1 and differentiation-associated proteins filaggrin and occludin, have been associated with a reduction in UV-mediated apoptosis (Dusek *et al.*, 2006; Mildner *et al.*, 2010; Rachow *et al.*, 2013). Filaggrin loss also results in increased UV-induced DNA damage (Mildner *et al.*, 2010). In the present study increased Erk phosphorylation was observed at the same UVB dosages where differentiation markers were reduced, consistent with the idea that surviving cells that do not undergo differentiation activate Erk pathway-mediated pro-proliferative signaling (Dumesic *et al.*, 2009). Treatment of organotypic cultures with TSA reduced UVB-induced

phosphorylation of Erk while promoting expression of Dsg1 and associated differentiation proteins. We propose that therapeutically increasing expression of Dsg1 to promote restoration of differentiation markers (Getsios *et al.*, 2009) as well as to repress pro-oncogenic EGFR/MAPK/ras signaling (Getsios *et al.*, 2009; Hammers and Stanley, 2013; Harmon *et al.*, 2013) may help prevent skin carcinogenesis.

In addition to skin cancer, UV exposure can initiate or exacerbate the pathology of other human skin diseases. For example, UV exposure induces acantholysis in the uninvolved skin of patients with pemphigus foliaceus, pemphigus vulgaris, and pemphigus erythematosus, disorders caused by auto-antibodies against Dsg1 or Dsg3 (Cram and Winkelmann, 1965; Igawa *et al.*, 2004; Jacobs, 1965; Kawana and Nishiyama, 1990; Makino *et al.*, 2013; Reis *et al.*, 2000). This was posited to be due to increased IgG deposits in intercellular spaces within the UV-induced lesions (Cram and Fukuyama, 1972). However, Dsg1 levels or localization were not examined to determine whether UV exposure exacerbates pemphigus antibody-induced depletion of Dsg1 from desmosomes. Studies are warranted to understand how decreases in Dsg1, Dsc1, K1, and K10 following UVB exposure may contribute to the pathologies of these and other more common epidermal diseases like psoriasis and eczema. There are reports of psoriasis patients developing pemphigus lesions following phototherapy and the underlying mechanisms remain unexplained (Kwon *et al.*, 2011; Sanchez-Palacios and Chan, 2004).

Therapeutically stabilizing Dsg1 in UV-exposed skin through use of HDAC inhibitors or other drugs could reduce symptoms of patients suffering from several skin diseases as well as potentially preventing skin carcinogenesis. HDAC inhibitors are in clinical trials as anti-cancer

agents. Two have been approved by the Food and Drug Administration for use against cutaneous T cell lymphomas, and several are being explored for treating psoriasis (Khan and La Thangue, 2012; Shuttleworth *et al.*, 2010). Therefore, use of these agents to help restore epidermal differentiation after acute sun exposure may be feasible.

Materials and Methods:

Cell culture and retroviral transduction

NHEKs were isolated from neonatal foreskin by the Northwestern University Skin Disease Research Center (NUSDRC) as described (Halbert *et al.*, 1992). Cells were propagated in M154 medium supplemented with human keratinocyte growth supplement (HKGS, Life Technologies, Grand Island, NY, USA), 1,000× gentamycin/amphotericin B solution (Life Technologies), and 0.07 mM $CaCl_2$ (low calcium). Confluent keratinocyte monolayers were induced to differentiate by addition of 1.2 mM $CaCl_2$ (high calcium) in M154 in the absence of HKGS. LZRS-GFP, LZRS-Flag Dsg1, LZRS-miR Dsg1, and LZRS-miR Lamin (control) were generated as previously described (Getsios *et al.*, 2004; Getsios *et al.*, 2009). Keratinocytes were transduced with retroviral supernatants produced from Phoenix cells (provided by G. Nolan, Stanford University, Stanford, CA) as previously described (Getsios *et al.*, 2004; Simpson *et al.*, 2010a). For organotypic cultures, keratinocytes were seeded on collagen/fibroblast matrices and grown submerged in E medium supplemented with 5 ng/ml epidermal growth factor (EGF) for two days, then grown at the air–medium interface in E medium without EGF according to published protocols (Simpson *et al.*, 2010a; Simpson *et al.*, 2010b).

UVB exposure

Cells (in sufficient Phosphate Buffered Saline - PBS - to minimally cover the culture plate surface) or organotypic cultures (raised to the air/liquid interface) were irradiated under two TL20W/01 narrow band UVB bulbs with peak irradiance at 311 nm wavelength (Solarc Systems, Inc, Barrie, ON, Canada). The exposure time required to obtain UVB doses (J/m^2) was calculated by measuring $\mu W/cm^2$ using an ILT1400A photometer (International Light Technologies, Peabody, MA) calibrated by the manufacturer. The photometer is equipped with detectors to measure UVB and UVC and no UVC was emitted from the UVB bulbs. For a clinical comparison of UVB dosages used throughout this study, depending upon skin type (age, pigmentation, thickness), 4000 J/m^2 UVB is considered 1 Minimal Erythemal Dose (MED) (van der Vleuten *et al.*, 1996).

Antibodies and reagents

Mouse monoclonal antibodies used: P124 (anti–Dsg1 extracellular domain; Progen, Heidelberg, Germany); 27B2 (anti–Dsg1 cytodomain; Invitrogen), U100 (anti-Dsc1; Progen), HECD1 (anti–E-cadherin; Takara, Kyoto, Japan) and 4A4 (anti-p63; Santa Cruz Biotechnology, Dallas, TX). Rabbit polyclonal antibodies used: K1, K10, and loricrin (gifts from J. Segre, National Human Genome Research Institute, Bethesda, MD), 1905 (anti-Dsg3; gift from J. Stanley, University of Pennsylvania, Philadelphia, PA), C33E10 (anti-pERK; Cell Signaling Technology, Danvers, MA), anti-Erk1/2 (Promega, Madison, WI), H-137 (anti-p63; Santa Cruz Biotechnology) and GAPDH (glyceraldehyde-3-phosphate dehydrogenase; Sigma-Aldrich). Chicken polyclonal antibody used: Pg (1407; Aves Laboratories, Tigard, OR). Secondary antibodies for immunoblotting were goat anti–mouse, –rabbit, and –chicken peroxidase (Rockland; KPL,

Gaithersburg, MD). Secondary antibodies for immunofluorescence microscopy were goat anti–mouse, –rabbit, and –chicken linked to fluorophores of 488 nm and 568 nm (Alexa Fluor; Invitrogen).

Immunoblot analysis of proteins

Whole cell or organotypic culture lysates were collected in Urea-SDS buffer (8M Urea/ 1% Sodium dodecyl sulfate/ 60 mM Tris pH 6.8/ 5% β-mercaptoethanol/ 10% glycerol) and sonicated. Samples separated by SDS-PAGE were transferred to nitrocellulose, blocked in 5% milk/PBS, and probed with primary antibody in milk for 1 hour at room temperature. Secondary, HRP-conjugated antibodies diluted 1:5000 in milk were added to blots after washing with PBS. Protein bands were visualized using enhanced chemiluminescence and exposure to X-ray film.

Quantitative real-time PCR

RNA was isolated using the RNeasy Mini kit (Qiagen, Valencia, CA), according to the manufacturer's instructions. Total RNA concentrations were equalized between samples, and cDNA prepared using the Superscript III First Strand kit (Invitrogen). Quantitative PCR was performed using SYBR Green PCR master mix (Applied Biosystems) and gene-specific primers in a StepOnePlus instrument (Applied Biosystems). Calculations for relative mRNA levels were performed using the ΔΔCt method, normalized to GAPDH. Primers used: Dsg1F TCCATAGTTGATCGAGAGGTCAC, Dsg1R CTGCGTCAGTAGCATTGAGTATC, GAPDHF ACATCGCTCAGACACCATG, GAPDHR TGTAGTTGAGGTCAATGAAGGG.

ChIP

NHEKs were fixed with 1% formaldehyde and ChIP was performed using anti-p63 antibodies with rabbit IgG antibodies as a negative control. ChIP was performed as previously described (Antonini *et al.*, 2010). Real-time PCR was performed using the SYBR Green PCR master mix (Applied Biosystems) in an ABI PRISM 7500.

Primers used: -25kbDsg1F TCTCTCAACCTGCACTCAATCTG, -25kbDsg1R GGGAGGCTTCTCTGCGATTA, -60kbDsg1F GGGCAATGACATCCCTTGTT, -60kbDsg1R GGTGTGTTCTGCAAGTTCCACTT, -70kbDsg1F TTAAGCAAAACTAATGGACCACAGA -70kbDsg1R GCTCATGCATGTTCATATACAAACC.

Histology, indirect immunofluorescence microscopy

Organotypic cultures fixed in 10% neutral buffered formalin were embedded in paraffin blocks, cut into 5 μm sections, and H&E stained by the NUSDRC. For indirect immunofluorescence microscopy, slides were baked at 60^{o}C, de-paraffinized by xylenes, dehydrated with ethanol, rehydrated in PBS and permeablized by 0.5% Triton X-100 in PBS. Antigen retrieval was performed by incubation in 0.01 M Citrate buffer (pH 6.0) or 0.5 M Tris buffer (pH 8.0) at 95^{o}C for 15 minutes. Sections were blocked in 1% BSA/0.05% Tween/PBS for 30 minutes at 37^{o}C. Primary antibody incubation was carried out overnight at 4^{o}C in blocking buffer followed by washing in PBS. Secondary antibody incubation was carried out at 37^{o}C for 45 minutes followed by washing in PBS. Sections were stained with 4′,6-Diamidino-2-phenylindole (DAPI - Sigma-Aldrich) at a final concentration of 5 ng/μl at room temperature for 2 minutes followed by washing in PBS and water. Cover slips were mounted with ProLong Gold Antifade Reagent (Life Technologies). Images were obtained with a 40x PL Fluotar, NA 1.0 objective on a Leica DMR microscope using a charge-coupled device camera (Orca 100, model C4742-95,

Hamamatsu, Bridgewater, NJ) and MetaMorph 6.1 software (MDS Analytical Technologies, Union City, CA) for fluorescence or a Leica DFC320 digital camera and Photoshop software (Adobe Systems, Mountain View, CA) for H&E images.

TUNEL assay

Cells undergoing apoptosis 48 hours following UVB exposure were detected using the *in situ* Cell Death Detection Kit (Roche, Penzberg, Germany) according to the manufacturer's protocol. The total cells per microscopic field were detected using DAPI.

HDAC Inhibition

On the day of lifting to the air-liquid interface organotypic models were left unexposed or exposed to 1500 J/m2 UVB on ice. Beginning the next day organotypic cultures were left untreated or treated with Dimethyl sulfoxide (DMSO) (Sigma-Aldrich) or TSA (1 μmol/L, Sigma-Aldrich) for 4 hours daily. Cultures were harvested on day 4 after lifting. Confluent cells were unexposed or exposed to 2000 J/m^2 UVB immediately prior to switching to 1.2 mM $CaCl_2$ containing medium. The next day cells were either left untreated or treated with DMSO or TSA in fresh high calcium-containing medium and harvested 72 hours after calcium switch.

Conflicts of Interest:

The authors state no conflict of interest.

Acknowledgements:

This work was supported by NIH R01 AR041836 and CA122151 with partial support from AR43380 to KJG. Additional support was provided by the JL Mayberry endowment to KJG. The financial support of Telethon, Italy (GGP09230), of the European ERA-Net Research Program on Rare Diseases (E-Rare-2; Skindev), and of the Italian Association for Cancer Research (AIRC; IG5348) to CM is gratefully acknowledged. JLJ's salary was supported by a Research Career Development Award through the Dermatology Foundation and salary and some research supplies were supported by a NIH/NCI Ruth L. Kirschstein Training Grant through Northwestern University's Robert H. Lurie Comprehensive Cancer Center (T32 CA070085-14) "Signal Transduction in Cancer". ATA's stipend and some research supplies were supported through the Northwestern University Lurie Comprehensive Cancer Center's Continuing Umbrella of Research Experience (CURE) Summer Program for Underserved Students, a supplement to P30 CA060553. Additionally, this research was supported in part by resources provided by the Northwestern University Skin Disease Research Center (NIH/NIAMS 5P30AR057216-02). Any opinions, findings, and conclusions or recommendations expressed in this material are those of the authors and do not necessarily reflect the views of the Northwestern University Skin Disease Research Center or the NIH/NIAMS.

References:

Antonini D, Russo MT, De Rosa L, *et al.* (2010) Transcriptional repression of miR-34 family contributes to p63-mediated cell cycle progression in epidermal cells. *J Invest Dermatol* 130:1249-57.

Bayerl C, Taake S, Moll I, *et al.* (1995) Characterization of sunburn cells after exposure to ultraviolet light. *Photodermatol Photoimmunol Photomed* 11:149-54.

Bellei B, Mastrofrancesco A, Briganti S, *et al.* (2008) Ultraviolet A induced modulation of gap junctional intercellular communication by P38 MAPK activation in human keratinocytes. *Exp Dermatol* 17:115-24.

Bernerd F, Asselineau D (1997) Successive alteration and recovery of epidermal differentiation and morphogenesis after specific UVB-damages in skin reconstructed in vitro. *Dev Biol* 183:123-38.

Bernstein BE, Kamal M, Lindblad-Toh K, *et al.* (2005) Genomic maps and comparative analysis of histone modifications in human and mouse. *Cell* 120:169-81.

Courdavault S, Baudouin C, Charveron M, *et al.* (2005) Repair of the three main types of bipyrimidine DNA photoproducts in human keratinocytes exposed to UVB and UVA radiations. *DNA Repair (Amst)* 4:836-44.

Cram DL, Fukuyama K (1972) Immunohistochemistry of ultraviolet-induced pemphigus and pemphigoid lesions. *Arch Dermatol* 106:819-24.

Cram DL, Winkelmann RK (1965) Ultraviolet-induced acantholysis in pemphigus. *Arch Dermatol* 92:7-13.

Del Bino S, Vioux C, Rossio-Pasquier P, *et al.* (2004) Ultraviolet B induces hyperproliferation and modification of epidermal differentiation in normal human skin grafted on to nude mice. *Br J Dermatol* 150:658-67.

Dumesic PA, Scholl FA, Barragan DI, *et al.* (2009) Erk1/2 MAP kinases are required for epidermal G2/M progression. *J Cell Biol* 185:409-22.

Dusek RL, Getsios S, Chen F, *et al.* (2006) The differentiation-dependent desmosomal cadherin desmoglein 1 is a novel caspase-3 target that regulates apoptosis in keratinocytes. *J Biol Chem* 281:3614-24.

English DR, Armstrong BK, Kricker A, *et al.* (1998) Case-control study of sun exposure and squamous cell carcinoma of the skin. *Int J Cancer* 77:347-53.

Ferone G, Mollo MR, Thomason HA, *et al.* (2013) p63 control of desmosome gene expression and adhesion is compromised in AEC syndrome. *Hum Mol Genet* 22:531-43.

Gambichler T, Rotterdam S, Tigges C, *et al.* (2008) Impact of ultraviolet radiation on the expression of marker proteins of gap and adhesion junctions in human epidermis. *Photodermatol Photoimmunol Photomed* 24:318-21.

Getsios S, Amargo EV, Dusek RL, *et al.* (2004) Coordinated expression of desmoglein 1 and desmocollin 1 regulates intercellular adhesion. *Differentiation* 72:419-33.

Getsios S, Simpson CL, Kojima S, *et al.* (2009) Desmoglein 1-dependent suppression of EGFR signaling promotes epidermal differentiation and morphogenesis. *J Cell Biol* 185:1243-58.

Green KJ, Simpson CL (2007) Desmosomes: new perspectives on a classic. *J Invest Dermatol* 127:2499-515.

Halbert CL, Demers GW, Galloway DA (1992) The E6 and E7 genes of human papillomavirus type 6 have weak immortalizing activity in human epithelial cells. *J Virol* 66:2125-34.

Hammers CM, Stanley JR (2013) Desmoglein-1, differentiation, and disease. *J Clin Invest* 123:1419-22.

Harmon RM, Simpson CL, Johnson JL, *et al.* (2013) Desmoglein-1/Erbin interaction suppresses ERK activation to support epidermal differentiation. *J Clin Invest* 123:1556-70.

Holleran WM, Uchida Y, Halkier-Sorensen L, *et al.* (1997) Structural and biochemical basis for the UVB-induced alterations in epidermal barrier function. *Photodermatol Photoimmunol Photomed* 13:117-28.

Hung CF, Chiang HS, Lo HM, *et al.* (2006) E-cadherin and its downstream catenins are proteolytically cleaved in human HaCaT keratinocytes exposed to UVB. *Exp Dermatol* 15:315-21.

Igawa K, Matsunaga T, Nishioka K (2004) Involvement of UV-irradiation in pemphigus foliaceus. *J Eur Acad Dermatol Venereol* 18:216-7.

Jacobs SE (1965) Pemphigus Erythematosus and Ultraviolet Light. A Case Report. *Arch Dermatol* 91:139-41.

Kawana S, Nishiyama S (1990) Involvement of membrane attack complex of complement in UV-B-induced acantholysis in pemphigus. *Arch Dermatol* 126:623-6.

Khan O, La Thangue NB (2012) HDAC inhibitors in cancer biology: emerging mechanisms and clinical applications. *Immunol Cell Biol* 90:85-94.

Koster MI (2010) p63 in skin development and ectodermal dysplasias. *J Invest Dermatol* 130:2352-8.

Kouwenhoven EN, van Heeringen SJ, Tena JJ, *et al.* (2010) Genome-wide profiling of p63 DNA-binding sites identifies an element that regulates gene expression during limb development in the 7q21 SHFM1 locus. *PLoS Genet* 6:e1001065.

Kwon HH, Kwon IH, Chung JH, *et al.* (2011) Pemphigus Foliaceus Associated with Psoriasis during the Course of Narrow-Band UVB Therapy: A Simple Coincidence? *Ann Dermatol* 23:S281-4.

Kwon OS, Yoo HG, Han JH, *et al.* (2008) Photoaging-associated changes in epidermal proliferative cell fractions in vivo. *Arch Dermatol Res* 300:47-52.

Lavker RM, Gerberick GF, Veres D, *et al.* (1995) Cumulative effects from repeated exposures to suberythemal doses of UVB and UVA in human skin. *J Am Acad Dermatol* 32:53-62.

Lee DS, Quan G, Choi JY, *et al.* (2005) Chronic ultraviolet radiation modulates epidermal differentiation as it up-regulates transglutaminase 1 and its substrates. *Photodermatol Photoimmunol Photomed* 21:45-52.

Lee JH, An HT, Chung JH, *et al.* (2002) Acute effects of UVB radiation on the proliferation and differentiation of keratinocytes. *Photodermatol Photoimmunol Photomed* 18:253-61.

Li D, Turi TG, Schuck A, *et al.* (2001) Rays and arrays: the transcriptional program in the response of human epidermal keratinocytes to UVB illumination. *FASEB J* 15:2533-5.

Lorincz AL (1960) Physiological and pathological changes in skin from sunburn and suntan. *JAMA* 173:1227-31.

Makino T, Seki Y, Hara H, *et al.* (2013) Induction of Skin Lesions by Ultraviolet B Irradiation in a Case of Pemphigus Erythematosus. *Acta dermato-venereologica*.

Matsumura Y, Ananthaswamy HN (2004) Toxic effects of ultraviolet radiation on the skin. *Toxicol Appl Pharmacol* 195:298-308.

Mildner M, Jin J, Eckhart L, *et al.* (2010) Knockdown of filaggrin impairs diffusion barrier function and increases UV sensitivity in a human skin model. *J Invest Dermatol* 130:2286-94.

Murakami T, Fujimoto M, Ohtsuki M, *et al.* (2001) Expression profiling of cancer-related genes in human keratinocytes following non-lethal ultraviolet B irradiation. *J Dermatol Sci* 27:121-9.

Pfeifer GP, Besaratinia A (2012) UV wavelength-dependent DNA damage and human non-melanoma and melanoma skin cancer. *Photochem Photobiol Sci* 11:90-7.

Provost N, Moreau M, Leturque A, *et al.* (2003) Ultraviolet A radiation transiently disrupts gap junctional communication in human keratinocytes. *Am J Physiol Cell Physiol* 284:C51-9.

Rachow S, Zorn-Kruppa M, Ohnemus U, *et al.* (2013) Occludin is involved in adhesion, apoptosis, differentiation and ca(2+)-homeostasis of human keratinocytes: implications for tumorigenesis. *PLoS One* 8:e55116.

Reis VM, Toledo RP, Lopez A, *et al.* (2000) UVB-induced acantholysis in endemic Pemphigus foliaceus (Fogo selvagem) and Pemphigus vulgaris. *J Am Acad Dermatol* 42:571-6.

Robert M, Bissonauth V, Ross G, *et al.* (1999) Harmful effects of UVA on the structure and barrier function of engineered human cutaneous tissues. *Int J Radiat Biol* 75:317-26.

Rosario R, Mark GJ, Parrish JA, *et al.* (1979) Histological changes produced in skin by equally erythemogenic doses of UV-A, UV-B, UV-C and UV-A with psoralens. *Br J Dermatol* 101:299-308.

Rundhaug JE, Hawkins KA, Pavone A, *et al.* (2005) SAGE profiling of UV-induced mouse skin squamous cell carcinomas, comparison with acute UV irradiation effects. *Mol Carcinog* 42:40-52.

Sabo PJ, Kuehn MS, Thurman R, *et al.* (2006) Genome-scale mapping of DNase I sensitivity in vivo using tiling DNA microarrays. *Nat Methods* 3:511-8.

Sanchez-Palacios C, Chan LS (2004) Development of pemphigus herpetiformis in a patient with psoriasis receiving UV-light treatment. *J Cutan Pathol* 31:346-9.

Sesto A, Navarro M, Burslem F, *et al.* (2002) Analysis of the ultraviolet B response in primary human keratinocytes using oligonucleotide microarrays. *Proc Natl Acad Sci U S A* 99:2965-70.

Shuttleworth SJ, Bailey SG, Townsend PA (2010) Histone Deacetylase inhibitors: new promise in the treatment of immune and inflammatory diseases. *Curr Drug Targets* 11:1430-8.

Simpson CL, Kojima S, Cooper-Whitehair V, *et al.* (2010a) Plakoglobin rescues adhesive defects induced by ectodomain truncation of the desmosomal cadherin desmoglein 1: implications for exfoliative toxin-mediated skin blistering. *Am J Pathol* 177:2921-37.

Simpson CL, Kojima S, Getsios S (2010b) RNA interference in keratinocytes and an organotypic model of human epidermis. *Methods Mol Biol* 585:127-46.

van der Vleuten CJ, Kroot EJ, de Jong EM, *et al.* (1996) The immunohistochemical effects of a single challenge with an intermediate dose of ultraviolet B on normal human skin. *Arch Dermatol Res* 288:510-6.

Yuki T, Hachiya A, Kusaka A, *et al.* (2011) Characterization of tight junctions and their disruption by UVB in human epidermis and cultured keratinocytes. *J Invest Dermatol* 131:744-52.

Figure legends:

Figure 1: **Acute UVB exposure of keratinocytes prior to induction of differentiation results in decreased expression of differentiation-associated proteins:** a) Immunoblots showing differentiation-associated proteins reduced in NHEKs exposed to UVB prior to inducing differentiation. Numbers under immunoblots represent band intensity fold change from no UVB control after normalization to GAPDH. b) Level of cell death induced by UVB dosages utilized throughout this study assessed using either the TUNEL assay or by counting the total number of cells per microscopic field 48 hours after UVB exposure.

Figure 2: **Dsg1 promotes epidermal differentiation and architectural recovery after UVB exposure:** a) Immunoblots showed that shRNA-mediated depletion of Dsg1 further reduced Dsc1, K10, and K1 compared to control NHEKs exposed to UVB prior to calcium switch. Numbers represent band intensity fold change from unexposed shCon-infected cells after normalization to GAPDH. b) Dsg1 depletion altered the architecture of UVB-exposed organotypic models compared to controls (H&E). Organotypic models were grown for 6 days before mock exposure or irradiation with 1000 J/m^2 UVB then harvested 1 or 7 days later. Bars = 50 μm. c) Dsc1, K10, and K1 proteins were expressed at higher levels when Dsg1 was ectopically expressed in UVB-exposed differentiating NHEKs compared to controls. Numbers represent band intensity fold change from unexposed GFP-infected cells after normalization to GAPDH.

Figure 3: **UVB-induced delay in differentiation and reduced Dsg1 mRNA levels are associated with decreased binding of p63 to regulatory regions upstream of the Dsg1 gene:** a-b) Initiation of Dsg1, Dsc1, K1, and K10 protein expression was delayed following exposure to UVB compared to unexposed control NHEKs. c) Dsg1 transcript levels remained reduced up to 72 hours in NHEKs following UVB exposure (2000 J/m^2 prior to calcium switch to induce differentiation) compared to unexposed controls. d) The binding of p63 to an enhancer regulatory region -60kB from the Dsg1 gene was reduced following UVB exposure. NHEKs were unexposed or exposed to 2000 J/m^2 UVB prior to calcium switch then harvested 29 or 48 hrs later and processed for ChIP. Immunoblot shows total p63 levels after UVB exposure.

Figure 4: **Treatment of epidermal models with the HDAC inhibitor TSA increases differentiation marker expression after UVB exposure:** a) Organotypic models were unexposed or exposed to 1500 J/m^2 UVB prior to lifting to the air-liquid interface, left untreated or treated with DMSO or TSA for 4 hours daily starting 24 hours later, then harvested 4 days after lifting. Numbers represent band intensity fold change comparing unexposed treated and untreated cultures and comparing UVB-exposed treated and untreated cultures after normalization to GAPDH. Immunoblots revealed that TSA treatment helped restore Dsg1, Dsc1, and K10 expression after UVB exposure. b) TSA treatment reduces phosphorylated Erk in UVB-exposed organotypic cultures compared to DMSO treated controls.

a

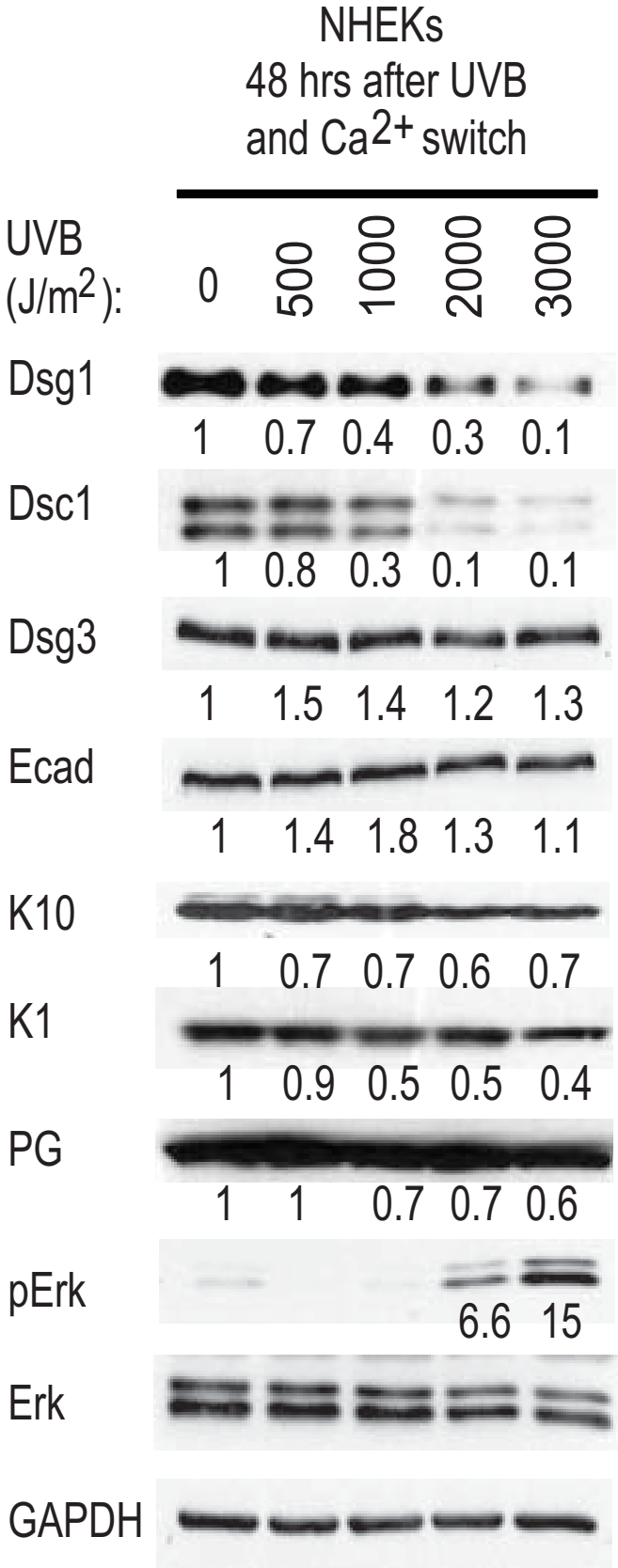

b

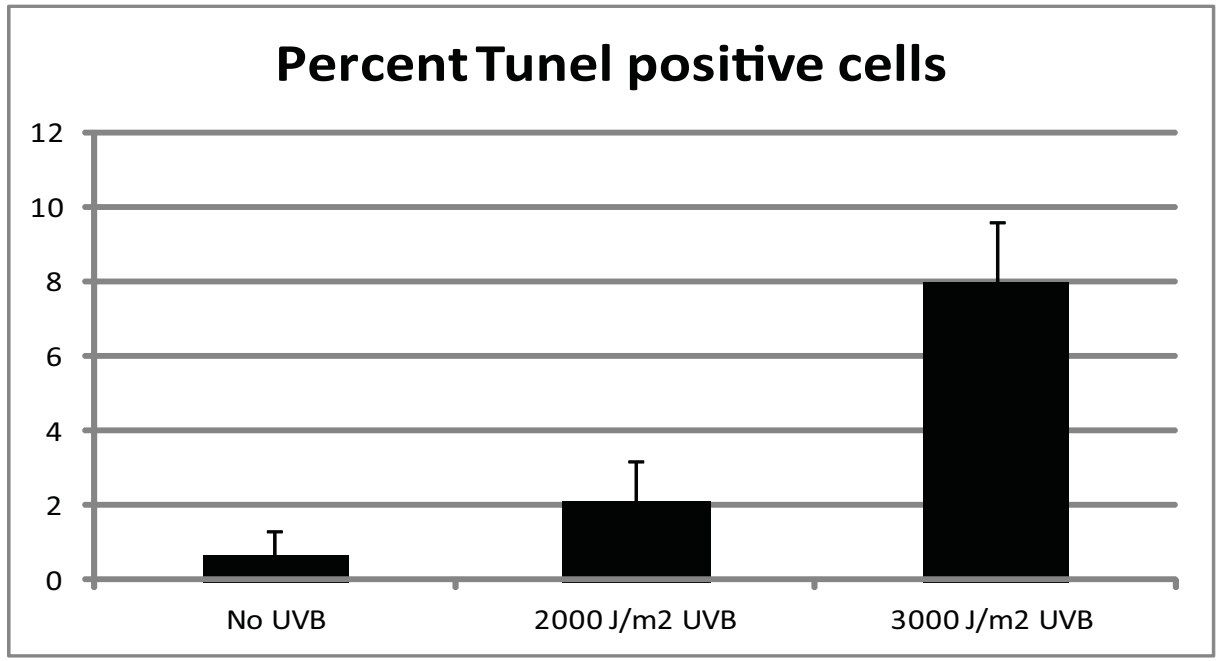

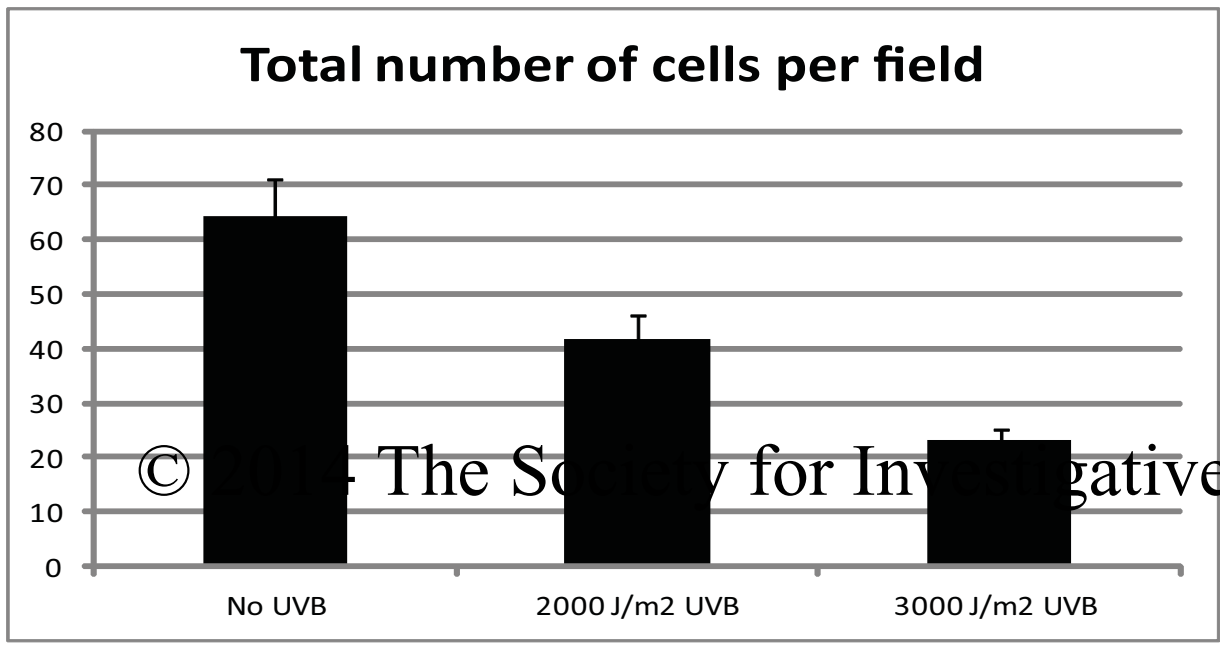

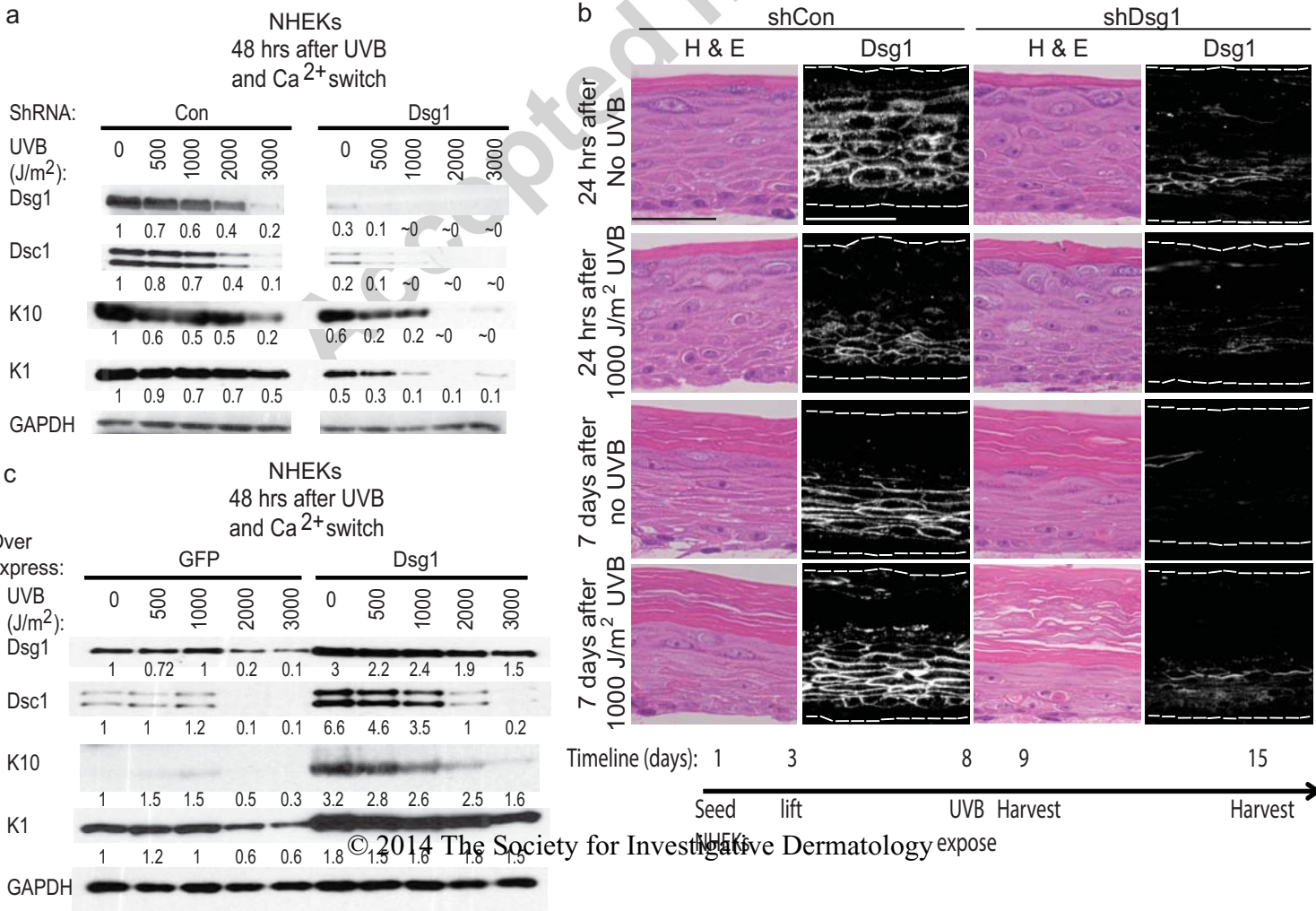

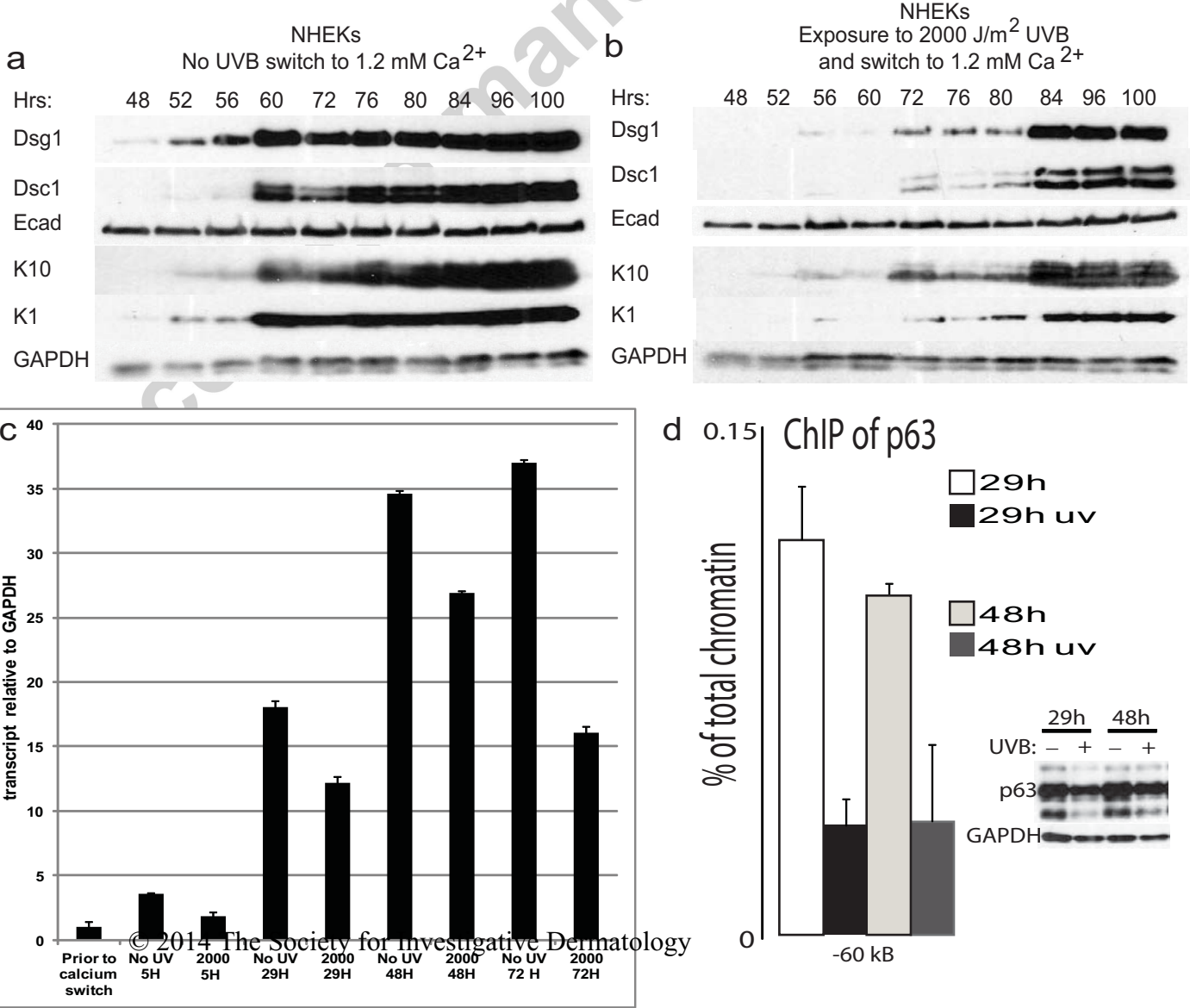

a

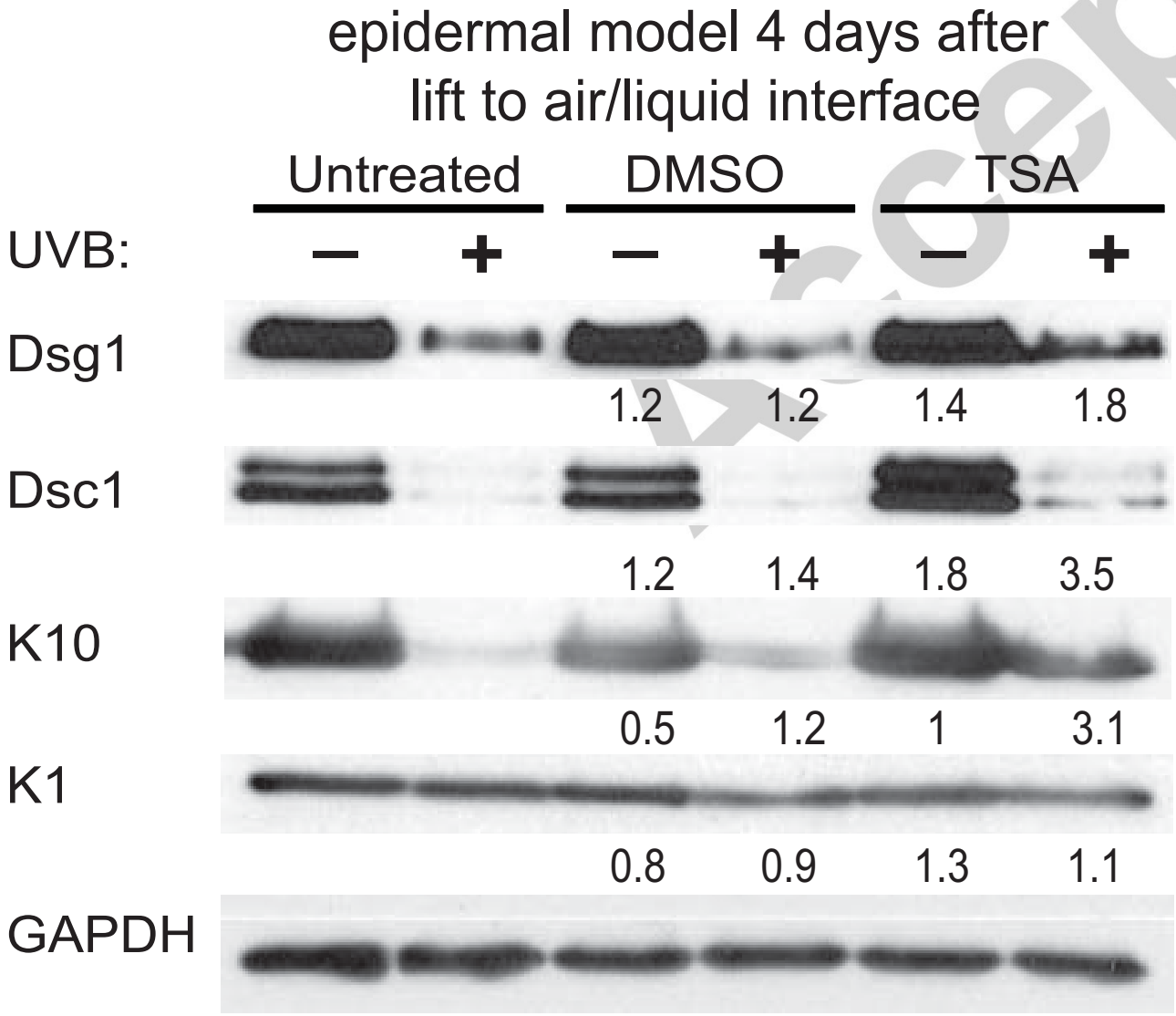

b